Detection of Biological Agents

Charles A. Primmerman

Biological weapons pose a real and potentially immediate threat. They are relatively cheap to manufacture and employ, and they have tremendous potential impact as terror weapons. These features make biological weapons attractive to rogue states and terrorist organizations. In this article we briefly describe the threat of biological weapons. We then describe Lincoln Laboratory work in developing advanced sensors to help combat the threat of biological weapons. These sensors include an early-warning sensor that can sense small quantities of biological particles in the air and issue an alarm in less than one minute and a bioelectronic identifying sensor that can potentially identify a biological agent from a single sensed particle.

Biological weapons have seldom been used throughout history [1–4]. The Biological and Toxin Weapons Convention of 1972 outlawed the possession and use of biological weapons; this convention has been ratified by all but a handful of major nations [5], and no nation has an overt, declared biological-weapons capability. Despite these facts, it appears that the threat of biological attack is increasing. Indeed, biological weapons may become the weapons of choice for rogue states and terrorist organizations.

Several factors contribute to this trend. First, the very horror associated with biological weapons serves to make them attractive to modern terrorist groups. Second, proliferation of biotechnology equipment and expertise has made it relatively easy to produce bioagents. Equipment needed to produce these bioagents can be found in pharmaceutical industries, food-processing plants, and even microbreweries. Such equipment is widely available on the open market. Likewise, there is a large, worldwide workforce trained in the basic techniques necessary to make biological weapons. The relative ease of making biological weapons is illustrated by the Iraqi program. (See the sidebar entitled "Iraq's Biological-Weapons Program.") Within only a few years Iraq clandestinely generated a substantial arsenal of biological weapons.

Third, small quantities of bioagents can cause huge numbers of casualties. For example, a lethal dose of anthrax spores is less than a microgram. Thus, less than 1 kg of anthrax would, if optimally distributed, be enough to give a lethal dose to every man, woman, and child in the United States. Even if not optimally distributed, relatively small amounts of bioagent can cause large numbers of casualties.

The World Health Organization estimated that attacking a large city with 50 kg of anthrax spores would produce 95,000 deaths and an additional 125,000 sicknesses [6]. The U.S. Congressional Office of Technology Assessment estimated that an attack on Washington, D.C., with 100 kg of anthrax spores would produce one to three million deaths [7]. The estimated casualties vary over a wide range because, fortunately, we have no empirical data on such an attack. Whichever estimate is accepted, casualties in a biological attack could be impressively large.

Finally, the combination of the relative ease of production of biological weapons and the potentially large number of casualties they can cause makes the biological weapon the "poor-man's" weapon of mass destruction. A relatively poor, technologically unsophisticated nation may well believe that developing biological weapons offers an advantage over an otherwise militarily superior adversary. Likewise, a terrorist organization can believe that the threat or actual use of biological weapons will gain them what more conventional acts of violence have not.

Components of Biological-Warfare Defense

Successfully defending against the threat of biological

IRAQ'S BIOLOGICAL-WEAPONS PROGRAM

IRAQ'S BIOLOGICAL-weapons program provides a case study in the threat posed by a rogue nation. It shows both how readily biological weapons can be developed and how easily their development can be hidden.

At the time of the Gulf War in 1991 it was widely suspected that Iraq had an offensive biological-warfare capability. Following the war, in response to U.N. Security Council resolutions requiring Iraq to disclose all weapons of mass destruction, Iraq maintained that it had only a tiny, defensive biological warfare effort of only about ten persons.

The U.N. Special Commission (UNSCOM) charged with obtaining information on Iraq's weapons of mass destruction and monitoring their destruction had hints and suspicions about a significant Iraqi offensive program. In four years of efforts, however, including intrusive inspections of approximately eighty potential dual-use biotechnology facilities in Iraq, UNSCOM was not able to obtain definitive proof of an Iraqi offensive biological-weapons program. Only after the August 1995 defection of General Hussein Kamel Hassan, who had (among other responsibilities) been in charge of the Iraqi biological-weapons program, was Iraq forced to reveal the extent of its program. (In revealing the program, Iraq claimed "Hassan had, unbeknownst to the senior level of the Iraqi leadership, hidden information on the prohibited programmes" [1].)

In late 1995 Iraq admitted to having conducted a major offensive biological-weapons program. This program, spread across many different sites, involved research into various bioagents, production of large quantities of certain bioagents, field testing of bioagents, and actual weaponization. Iraq claimed that its program began in 1985 and that production and weaponization work accelerated dramatically in August 1990, coinciding with the invasion of Kuwait. Given the Iraqi claims, UNSCOM concluded that in five years, "the achievements of Iraq's biological weapons program were remarkable" [1].

Iraq admitted to producing 8500 liters of anthrax and 19,000 liters of concentrated botulinum toxin. It also claimed to have made 7200 liters of aflatoxin, which remains intriguing, for although aflatoxin is a known carcinogen, it does not appear to be an appropriate bioagent. These and all Iraqi numbers on biological weapons should be regarded as suspect; subsequent UNSCOM investigations concluded that the Iraqi methodologies for calculating most numbers were seriously flawed and that verification is impossible because of destroyed documents [2].

Iraq also admitted to working on ricin (a toxin produced from castor beans), clostridium perfringins (gas gangrene), and three viruses: hemorrhagic conjunctivitis, a rotavirus, and camel pox. It also developed an anti-crop bioagent—wheat smut, which was produced in large quantities and used in field tests.

Iraq claimed to have made bioagents into weapons on various platforms. One hundred R400 (400 lb) bombs were filled with botulinum toxin, fifty with anthrax spores, and sixteen with aflatoxin. Twenty-five special Al Hussein missile warheads were built after August 1990; thirteen were filled with botulinum toxin, ten with anthrax, and two with aflatoxin. These weapons were deployed at four sites during the Gulf War, and authority to use the weapons was delegated to field commanders.

Iraq performed field trials of bioagents in 155-mm-artillery shells and in 122-mm rockets. It also tested a delivery technique using a 2000-liter tank and a sprayer mounted on a remotely piloted aircraft [3].

Iraq claims that in 1991, following the war, it destroyed all filled biological munitions and all stocks of bioagents. This unilateral destruction was, itself, in vio-

lation of U.N. Security Council resolutions, and the claimed destruction remains unverified. After Iraq admitted its offensive biological-warfare program, certain facilities, including the major production plant at Al Hakam, were destroyed under UNSCOM supervision.

Before being expelled from Iraq, UNSCOM concluded that Iraq had continued to conceal facts regarding its biological-warfare program [4]. Given this concealment, which is even easier in the absence of UNSCOM inspectors, it is reasonable to presume that components of the program still exist, if not actual weapons, then certainly seed stocks of bioagents and manufacturing recipes. Because much of the required equipment still exists as dual-use biotechnology equipment and because the trained workforce still exists, it is likely that Iraq could reconstitute a biological-warfare capability in a relatively short time.

References

1. United Nations Security Council, "Report of the Secretary General on the Status of the Implementation of the Special Commission's Plan for the Ongoing Monitoring and Verification of Iraq's Compliance with Relevant Parts of Section of Security Council Resolution 687 (1991)," S/1995/864 (11 Oct. 1995), <http://www.un.org/Depts/unscom/sres95-864.htm>.
2. United Nations Security Council, "Report of the Executive Chairman on the Activities of the Special Commission Established by the Secretary-General Pursuant to Paragraph 9 (b) (i) of Resolution 687 (1991)," S/1998/332 (16 Apr. 1998), <http://www.un.org/Depts/unscom/sres98332.htm>.
3. R.A. Zilinskas, "Iraq's Biological Weapons: The Past as Future?" *J. Am. Med. A.* **278** (5), pp. 418–424.
4. United Nations Security Council, "Report of the Executive Chairman on the Activities of the Special Commission Established by the Secretary-General Pursuant to Paragraph 9 (b) (i) of Security Council Resolution 687 (1991), S/1998/920, (6 Oct. 1998), <http://www.un.org/Depts/unscom/sres98-920.htm>.

weapons requires vigorous efforts in many areas. Figure 1 shows the five principal components of biological defense: (1) deterrence and destruction—stopping the enemy before he has used biological weapons, (2) protection—masks and air filters, (3) decontamination after an attack, (4) medical countermeasures—both immunization before an attack and treatment after an attack, and (5) detection and warning.

Detection is the keystone of biological defense. Without detection of an attack there will be no warning to don protective masks. Without detection there will be no knowledge of what to decontaminate or when it is fully decontaminated. Without detection prompt, specific medical treatment will not be possible.

Before an attack a slightly different kind of detection is essential. Detecting what a potential enemy is manufacturing enables deterrent activity. It also enables appropriate immunization programs.

Lincoln Laboratory efforts in biological-agent defense have concentrated on detection and warning. We have been developing sensors and sensor systems to provide highly sensitive real-time detection, discrimination, and identification of bioagents.

A Biological Attack

To detect and defend against a biological attack, we must understand its general nature. A biological attack can take on many forms depending on what bioagent is used, how it is dispersed, and what is attacked.

Biological weapons can be used to attack human beings, livestock, or crops. We have focused our detection efforts on defending humans against biological attacks. We note, however, that attacks on livestock and crops could have significant strategic value, and thus should not be ignored. Indeed, Iraq made both anti-livestock and anti-crop bioagents into weapons.

The potential scale of a biological attack on human beings spans a wide range. A biological weapon can be used to kill a single individual, or it can be dispersed over a major city to kill millions of people. In between these extremes, one can imagine biological weapons being used to attack concentrations of persons in various military and civilian settings: an air base, a large office building, an aircraft carrier, a sports stadium, a military staging area, a subway. In

our detection efforts we will assume that the attack is against some substantial number of persons.

Bioagents can be disseminated in at least three major ways: by vector (i.e., insects), by contaminating water or food supplies, and by distributing them as aerosol particles in the air. Well-known virulent diseases are normally transmitted by insects (for instance, fleas transmit plague and mosquitoes transmit yellow fever), and the use of insects in biological warfare has apparently been tested [8]. Nevertheless, the difficulty of dealing with large numbers of insects and their unpredictability once released make significant biological attacks with insects seem unlikely.

Disease and death from contaminated water and food are also well known in nature. For example, typhoid fever is transmitted by contaminated water, and botulism commonly comes from eating improperly canned food. Using biological weapons to contaminate water or food may be an effective way to murder one person or a few persons, but it is unlikely to be effective in infecting large numbers of persons. Consider, for instance, the problems of putting bioagents in a municipal water supply, which at first glance might seem an effective method. First, large quantities of bioagent would be needed because the bioagent would be diluted in a large water supply. Second, municipal water supplies are almost universally treated (e.g., with chlorine) to kill harmful bacteria and viruses.

By far the most effective method for a biological attack is to dispense the bioagent as aerosol particles in the air. The bioagent particles then float in the air until they are inhaled. Aerosol attacks have two major advantages: (1) the bioagent particles are naturally dispersed in the atmosphere and, driven by the wind, can drift over large areas, and (2) many diseases are more virulent when spread by the aerosol route. For maximum effect it is generally agreed that the bioagent particles should be in the size range of 1 to 10 μm. Larger particles will precipitate out of the air in too short a time; smaller particles will tend to be expelled from the lungs.

Aerosol particles can be generated in various ways. Perhaps the simplest way is to employ a sprayer of the kind used with insecticides. Such a sprayer could be carried by an individual or mounted in a truck or aircraft. Biological weapons can also be dispersed by bombs, missiles, and artillery shells.

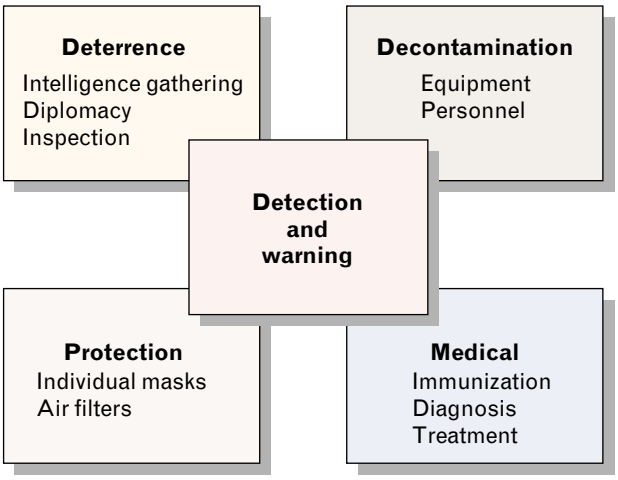

FIGURE 1. The five principal components of biological defense. Detection and warning constitute the keystone.

Bioagents tend to decay rapidly when exposed to ultraviolet light; thus attacks at night are more effective than in the daytime. Ideal meteorological conditions for an attack would include an inversion layer, to keep the bioagent cloud trapped near the earth's surface, and moderate steady winds of about 5 to 15 kt. These are the conditions a logical, rational attacker might choose; but given that the use of biological weapons could be considered, *ipso facto*, proof of irrationality, it would be unwise to assume that biological weapons will only be used under optimum conditions. We should be prepared for biological attacks under a wide range of conditions.

Bioagents

Possible bioagents fall into five categories: (1) bacteria, (2) rickettsiae (which are similar to bacteria), (3) viruses, (4) fungi, and (5) toxins of biological origin. Toxins are, in fact, more like chemical agents in that they are not living organisms and do not reproduce in the human body; nevertheless, they are normally included as bioagents.

The list of candidate bioagents is actually remarkably short. For instance, the Australia Group—a confederation of nations concerned with the proliferation of chemical and biological weapons—has fewer than fifty possible bioagents on its primary list [8]. Genetic

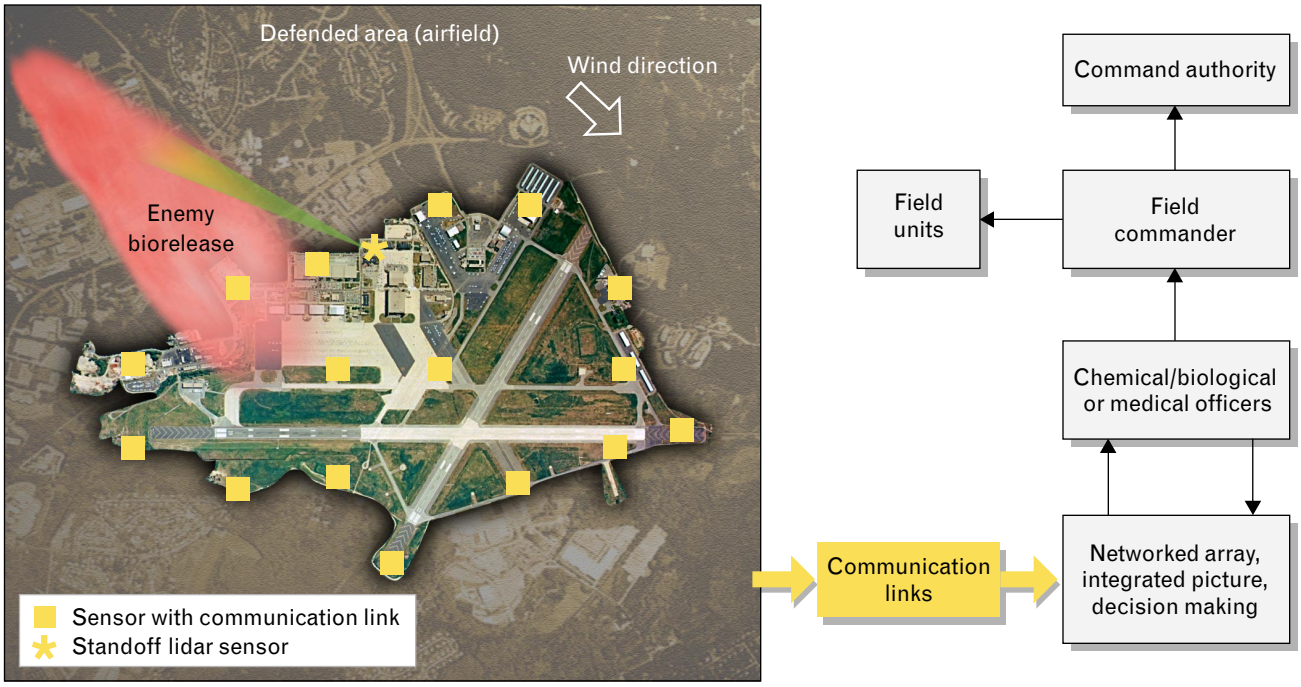

FIGURE 2. Nominal detection architecture for defense of a military airfield against a biological attack. The sensor network includes stationary point sensors, mobile point sensors, and a standoff lidar sensor. All sensor information is networked together to present an integrated picture to chemical/biological or medical officers.

engineering could, of course, vastly increase the number of potential bioagents.

To be an efficacious bioagent an organism must satisfy six broad criteria. It must (1) be relatively easy to manufacture in sufficient quantity, (2) be storable for months or years without significant degradation, (3) be disseminatable as a 1-to-10-μm aerosol, (4) survive dissemination effects (e.g., from a bomb), (5) survive for hours in the air without degradation, and (6) cause appropriate effects in its intended victims.

Note that there can be considerable variation in what an attacker considers appropriate effects. For instance, in a wartime tactical use of bioagents an attacker may prefer a fast-acting toxin; in a terrorist act the attacker may prefer a bioagent with a long gestation period. A military user will likely not want a bioagent that could cause an epidemic among his own people and thus, might prefer an epidemic-causing, contagious bioagent for the additional panic and disruption it could cause.

Darryl P. Greenwood at Lincoln Laboratory conducted a study to assess the bioagents most likely to be employed by a military user. The most likely bioagents and some of their characteristics are given in Table 1, which is derived from Greenwood's study. The bioagent characteristics in Table 1 have been scored from the point of view of the biological attacker: green is good for the attacker; red is bad for the attacker; yellow is either fair for the attacker or represents an emerging threat worth watching. Note that what is good and bad can change depending on the attacker's mission. Thus, we have scored high fatality rate as good, but some attackers may prefer a bioagent that is only incapacitating. As a natural bioagent, anthrax is clearly in a class by itself; it leads virtually everyone's bioagent threat list. (See the sidebar entitled "Anthrax as a Bioagent.")

Detection System Architecture

Figure 2 shows a detection architecture for defending a military port against a bioagent attack. The defended area is a military airfield, but the arrangement would be similar for a seaport, staging area, or other military installation. There would be a network of point sensors distributed around the airfield. Most of these sensors would be at the perimeter fence, but

Table 1. Likely Biological Agents and Their Characteristics

Bacteria and Rickettsiae

Disease	*# Cells to Infect*	*Incubation (days)*	*Vaccine Availability*	*Intervention (days)*	*Epidemic Risk*	*Fatality Risk*	*Treatability**
Anthrax	10,000	1–7	Yes	0.5–1	None	High	Yes†
Pneumonic Plague	3000	1–6	Ineffective	0.5–1	High	High	Yes†
Tularemia	10–50	1–10	Yes	0.5–1	None	Moderate	Yes
Glanders, Meloidosis	Unknown	3–5	No	3	Low	Moderate	Yes
Brucellosis	1300	7–21+	No	1–7	None	Low	Yes
Q Fever	1–10	7–28	Yes	1–7	None	Very low	Yes
Psittacosis	Unknown	1–15	No	3–5	Low	Low	Yes
Rocky Mountain Spotted Fever	A few	2–10	Yes	2–7	None	Low	Yes

Viruses

Smallpox	A few	7–21	Yes	3–7	Moderate	High	No
Dengue	Unknown	2–7	In development	1–2	High	Very low	No
Equine Encephalitis (EE)	25‡	2–15	Experimental	2	Low	Low to high	No
Hantaan	Unknown	5–42	In development	2–4	Low	High	No
Congo-Crimean Hemorrhagic Fever	Unknown	1–2	Experimental	1–2	Low	High	No
Ebola	Unknown	2–21	No	0.5–2	Moderate	Very high	No
Lassa	Unknown	3–16	Experimental	1–2§	Low	Low	No

Biological Toxins

Disease/ Agent	*Fatal Dose (μg)*	*Onset (hours)*	*Antitoxin Availability*	*Intervention (hours)*	*Stability*	*Fatality Risk*	*Treatability*
Botulinum	0.1	1–72	Yes	0.5–1	Low	High	No
Staphylococcal Enterotoxin B	1–10	1–12	No	0.5–1	Moderate	Low	No
Perfringens	10–500	6–24	No	1–6	Moderate	Low to high	No
Ricin	100	8–12	In development	0.5–1	Moderate	High	No
Saxitoxin	~800	0.1–2+	No	0.2	Low	Low	No
Tetrodotoxin	~800	0.1–8	No	0.1	Low	Moderate	No
Aflatoxin	100,000	Very long	No	6	High	Long term	No

* With antibiotics; † If detected early; ‡ Refers to Venezuelan Equine Encephalitis; § According to anecdotal evidence.

ANTHRAX AS A BIOAGENT

ANTHRAX TOPS ALMOST everyone's list of diseases likely to be employed in biological warfare [1]. Anthrax, in common with several other biological-warfare diseases, is principally an animal disease; it mainly effects herbivores, such as cattle, sheep, and goats. Anthrax has been known and described since antiquity, dating back to at least the fifth Egyptian plague (c. 1500 B.C.). It remains pandemic in many parts of the world.

Anthrax is caused by the bacterium *Bacillus anthracis*, which was first isolated by Robert Koch in the 1870s. Koch used this bacterium to provide the first experimental proof for the germ theory of disease. The famous "Koch's postulates" for proving that a specific microorganism causes a specific disease came from his work with *Bacillus anthracis*.

A feature that makes *Bacillus anthracis* particularly attractive as a bioagent is that, when key nutrients are removed, the vegetative bacterium spontaneously develops into a dormant state known as a spore. An electron-microscopic picture of anthrax spores is shown in Figure A. Spores are rugged and resistant to various stresses such as heat, radiation, drying, and chemical disinfectants. In the spore state, bacteria can survive for at least decades and perhaps much longer. For example, during World War II the British conducted experiments with *Bacillus anthracis* spores on the Scottish island of Gruinard; the island remained contaminated with viable anthrax spores until it was decontaminated with formaldehyde and seawater in 1986.

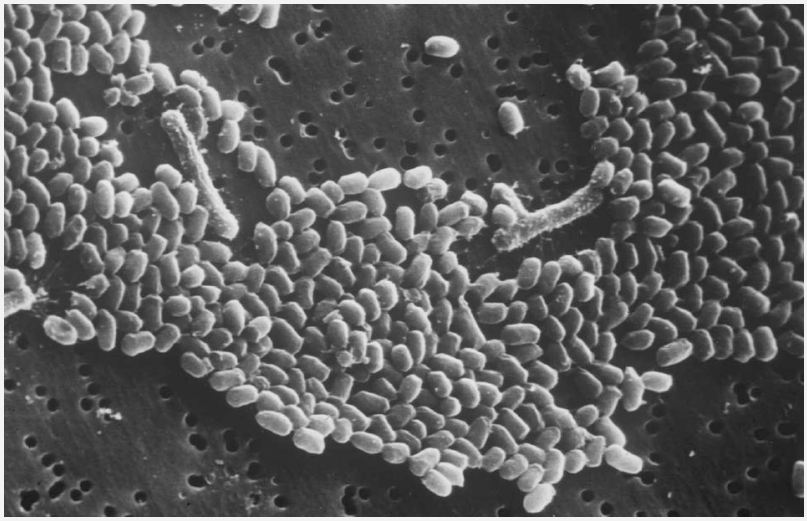

FIGURE A. Electron microscope picture of *Bacillus anthracis* spores. This picture was provided by John Ezzell at the U.S. Army Medical Research Institute for Infectious Diseases (USAMRIID).

Anthrax spores are relatively easy to manufacture, store, and dispense. The spores can infect humans by being inhaled. In fact, inhalation anthrax was once known as woolsorter's disease, because it affected those in the textile industry who handled wool from infected sheep.

After inhaling a sufficient dose of anthrax spores (8,000 to 50,000) a person typically begins to show fairly nonspecific cold or flu-like symptoms in one to five days. An untreated patient's death normally ensues in several days from severe respiratory distress. Anthrax, like most bacterial diseases, is treatable with antibiotics; to be effective, however, antibiotic treatment for anthrax must begin *before* symptoms occur. Vaccines are available, and in fact, all U.S. military personnel are being vaccinated against anthrax. Anthrax is not contagious from person-to-person; thus, an anthrax attack would not cause an epidemic.

Reference

1. J.C. Pile, J.D. Malone, E.M. Eitzen, and A.M. Friedlander, "Anthrax as a Potential Biological Warfare Agent," *Arch. Intern. Med.* **158** (5), 1998, pp. 429–434.

some would be placed in the center of the airfield. Robert W. Miller at Lincoln Laboratory performed a detailed analysis of this defensive network. His analysis showed that about fifty point sensors might be required for effective defense.

In addition to the emplaced point sensors, several similar sensors could be mounted on mobile platforms such as ground vehicles or unmanned air vehicles (UAVs). These vehicles could either patrol upwind of the airfield or be on call to respond if suspicious events occurred upwind. A lidar system could scan the area upwind of the airfield to provide standoff detection of any biological attack.

To provide an integrated picture of a possible biological attack, information from all the sensors would be transmitted over high-speed data links and integrated. Information from ancillary sensors, such as meteorological sensors, would also be included. All this information would be presented in a coherent way to the chemical/biological officer and the medical officer so that they could make informed decisions and alert the field commander. Automatic warning to troops could also be implemented.

The point sensors shown in Figure 2 would each comprise several subsystems, as shown in Figure 3. At the front end of the sensor system would be an early-warning (or trigger) sensor that continuously samples the air for suspicious events. The early-warning sensor would not identify specific bioagents, but it would be capable of classifying an aerosol cloud as a threat cloud or a nonthreat cloud. When the sensor detected a threat cloud, it would sound an alarm.

At the back end of the sensor system would be an identifier. This system would turn on when the early-warning sensor triggered an alarm. The identifier would precisely identify the bioagent to confirm the attack and guide the medical response.

Between the early-warning sensor and the identifier might be several stages of intelligent particle sampling and fluid preparation. These stages would take the airflow from the early-warning sensor and enrich and purify it, so that the identifier would have a sample high in suspicious particles and low in background dirt particles.

An architecture similar to that shown in Figure 2 could apply in civil defense against a possible terrorist attack. Figure 4 shows the architecture for defense of a building. Point sensors would be distributed throughout the building, particularly in air-handling ducts. First responders (e.g., firemen) could hand carry additional sensor units into the building. Again, all the sensors would be networked to give an integrated picture, in this case to civil authorities and medical personnel.

The sensor architectures shown in Figures 2 and 4 are designed to warn people before they receive infectious or toxic exposures so that they can take protective action. In most cases, a fairly simple mask will protect a person from a bioagent aerosol attack.

To be able to issue a timely warning to don masks, however, a sensor must operate rapidly and with high sensitivity. Sensitivity and time requirements for a sensor collocated with the persons it is protecting are shown in Figure 5. Figure 5 shows the bioagent con-

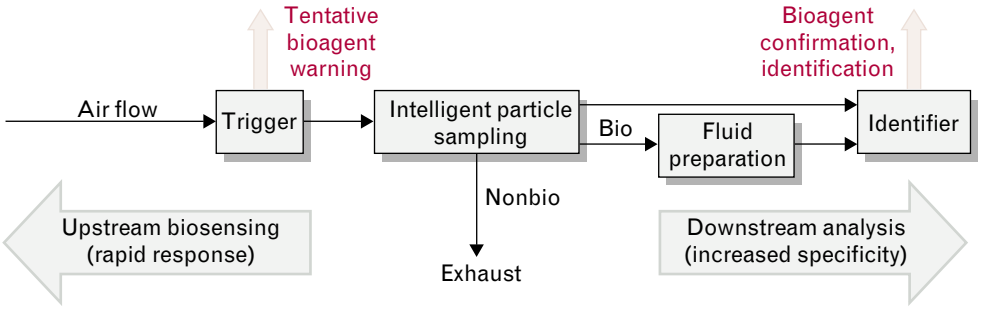

FIGURE 3. Block diagram of complete bioagent sensor. The front end is an early-warning trigger that constantly samples the air and rapidly issues an alarm (within a minute) if suspicious bioaerosols are detected. The back end is an identifier that is turned on by the trigger and precisely identifies the bioagent to confirm the attack and guide medical response. In between may be several stages of intelligent particle sampling and fluid preparation to enrich and purify the sample to enhance the performance of the identifier.

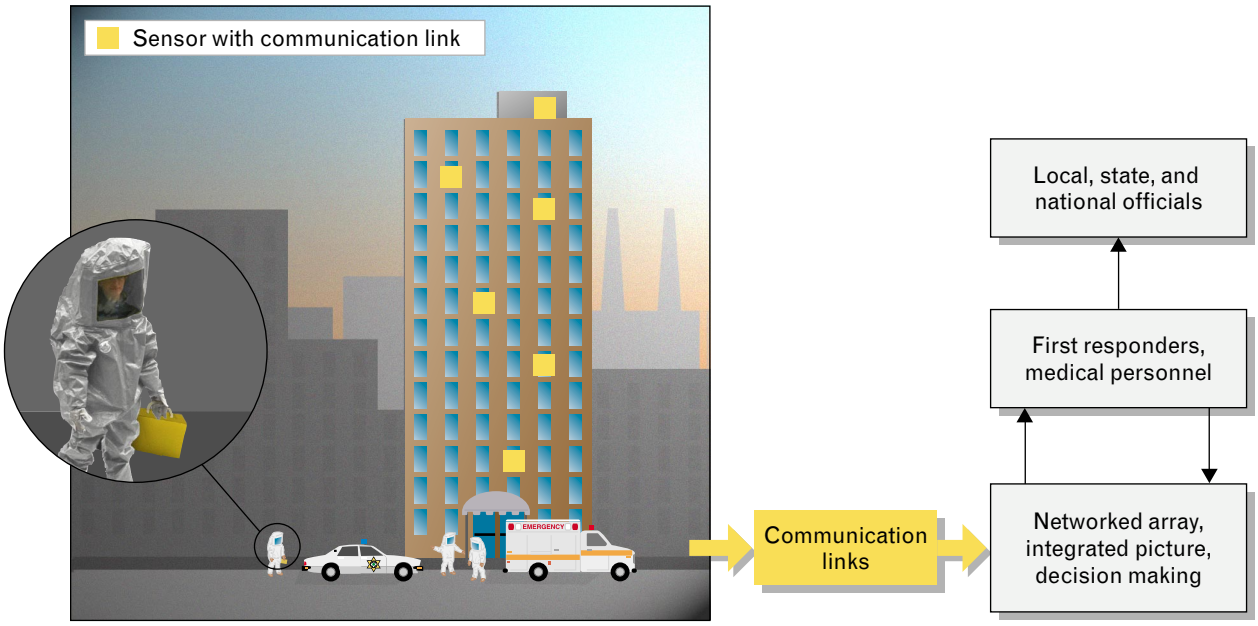

FIGURE 4. Nominal detection architecture for defense of a civilian building against a terrorist attack. The architecture eliminates the standoff lidar in the military-port architecture of Figure 2, but adds portable sensors hand carried by first responders. Sensor data are networked as in the military-port architecture, but the integrated information is now presented to civilian first responders, medical personnel, and other civilian officials.

centration needed for an unprotected person breathing at a normal rate to get an infectious dose, plotted against time for various potential bioagents. For example, at a concentration of 100 particles/liter of *Bacillus anthracis* (anthrax) a person would become infected in ten minutes. On the other hand, for *Francisella tularensis* (tularemia, or rabbit fever) at a concentration of only 10 particles/liter a person would become infected in less than a minute.

To protect a person from disease we need to detect and warn in less time than it takes to infect. Thus, our sensor goals are a sensitivity of 1 particle/liter or fewer and a detection time of less than one minute.

As anyone who has had a throat culture performed knows, most current medical lab techniques are in the upper right of the plot in Figure 5; that is, they take many hours to days and require many particles. These techniques, of course, are not "detect-to-warn" but are "detect-to-treat." Illness onset after a biological attack typically can take several days; thus, precise identification of the disease need not be as rapid as the initial warning to don masks. We note, however, that for many diseases (e.g., anthrax) treatment must begin before symptoms occur, or it is too late to prevent death. Rapid identification is, therefore, important to initiate appropriate medical treatment and to help reduce panic after an attack.

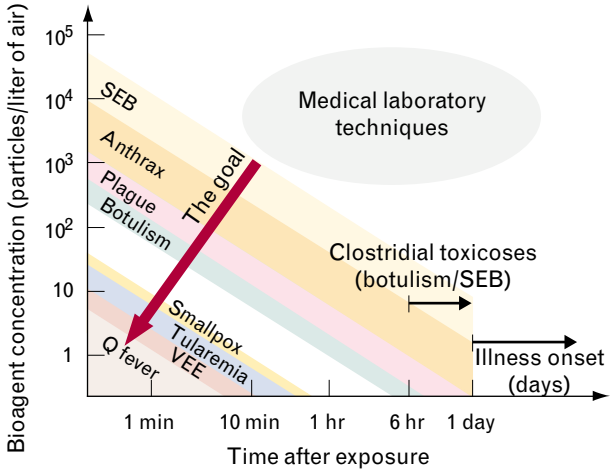

FIGURE 5. Requirements for a bioagent detector to protect personnel against infectious or toxic exposure. The required response time is plotted against the bioagent concentration for various bioagents. This plot assumes that the sensor is being used to warn a collocated, unprotected (i.e., unmasked) individual who is breathing at a normal rate of 10 to 20 liter/min). Note that SEB is staphylococcal enterotoxin B, and VEE is Venezuelan equine encephalitis.

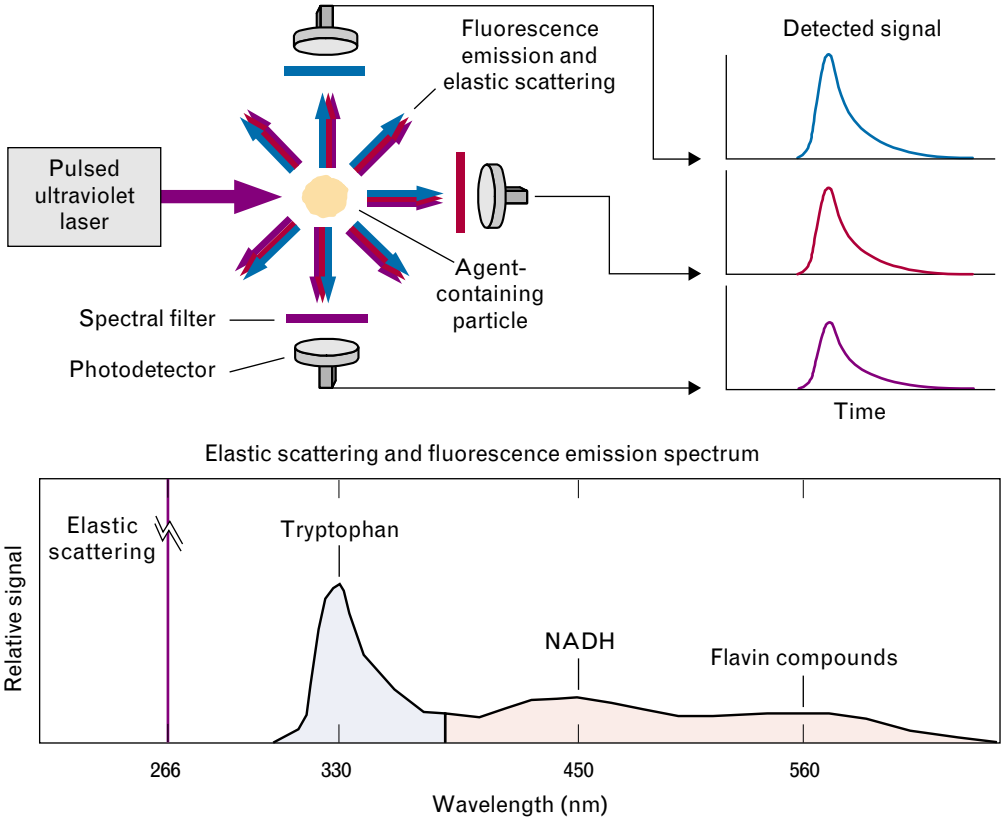

FIGURE 6. Concept for the Lincoln Laboratory biological-agent warning sensor (BAWS). Individual aerosol particles are illuminated by a pulsed ultraviolet laser operating at 266 nm. Light from the aerosol particle is detected in three channels: one at 266 nm, which measures the elastic scattering; a second between 300 and 400 nm, which measures the ultraviolet fluorescence from such substances as the amino acid tryptophan; and a third between 400 and 600 nm, which measures the visible fluorescence from such substances as NADH (the reduced form of nicotinamide adenine dinucleotide) and flavin compounds.

Biological-Agent Warning Sensor

Thomas H. Jeys at Lincoln Laboratory developed the concept for a novel biological agent warning sensor (BAWS) [9, 10] based on the principle of laser-induced fluorescence. Subsequently, he has led the development and field testing of several versions of this sensor. The function of this sensor is to provide early warning of the presence of suspicious biological particles in the air. Consequently, the BAWS sensor can discriminate suspicious particles from naturally occurring particles, such as pollen and mold spores, but it cannot identify specific bioagents. Identification is the function of another sensor, to be described later.

The BAWS concept of operation may be described with reference to Figure 6. A fan draws air into the sensor. Individual aerosol particles in the airstream are illuminated by a pulsed ultraviolet (UV) laser operating at 266 nm. Some of the light is scattered from the aerosol particle; some of the light is absorbed by the particle and rapidly reemitted at longer wavelengths in a process known as laser-induced fluorescence. Light from the particle is collected in three photomultiplier detectors. The first detector is spectrally filtered to collect only the scattered light at 266 nm; this detection signal is proportional to the particle's size. The second detector is spectrally filtered to collect UV light in the 300-to-400-nm range; this signal comes principally from biofluorescence of the amino acid tryptophan, which is found in almost all living organisms. The third detector is spectrally filtered to collect visible light in the 400-to-600-nm

range; this signal comes principally from biofluorescence of NADH (the reduced form of nicotinamide adenine dinucleotide) and flavin compounds, which are also found in living organisms.

The technique of using laser-induced fluorescence to detect bioaerosols is not novel; it has been known for more than two decades. Making this technique into a practical, high-performance sensor, however, has been made possible by two Lincoln Laboratory developments: (1) the passively Q-switched microlaser and (2) sophisticated processing for real-time discrimination.

The diode-pumped, passively Q-switched microlaser was invented by John J. Zayhowski [11–13]. This laser, shown in Figure 7, consists of an approximately 1-mm^3 Nd:YAG (neodymium-doped yttrium-aluminum-garnet) laser chip and a Cr:YAG (chromium-doped YAG) Q-switching chip. The laser is pumped through a fiber by a conventional 808-nm diode laser. The 1064-nm laser output is doubled to 532 nm by a KTP (titanate-phosphate) crystal and doubled again to 266 nm by a BBO (barium-borate) crystal. The final output at 266 nm consists of about 1-μJ, 500-psec pulses at a 10-KHz repetition rate. As shown in Figure 7, the entire laser assembly fits in a housing about as big as a person's thumb. The laser has no moving parts or adjustments and is extremely rugged. (In another implementation the laser was used in a pollution-monitoring system that was pounded into the ground in the head of a cone penetrometer [14].)

The small size and low power consumption of the microlaser enable us to build a compact, low-power bioaerosol sensor. The high-repetition rate of the laser enables us to interrogate individual aerosol particles at an effective sampling rate (about 20 liter/min) that exceeds normal human breathing rate.

The three detection channels permit us to discriminate threat aerosols from nonthreat aerosols. The discrimination processing may be described heuristically with reference to Figure 8, which shows four two-dimensional histograms for many measurements made with the BAWS. In each case the horizontal axis is the normalized difference between the UV and visible channels, and the vertical axis is the normalized difference between the UV and elastic channels. The number of particles for particular differences is indicated by color, with the red end of the spectrum denoting higher concentration and the violet end denoting lower concentration.

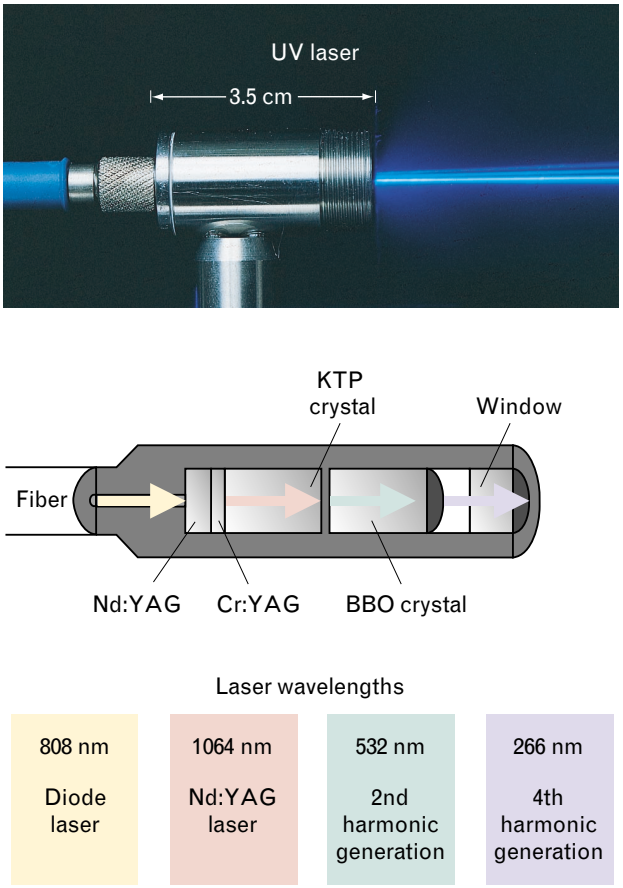

FIGURE 7. Diode-pumped, passively Q-switched microlaser. This laser, invented at Lincoln Laboratory, has been built in various configurations. In the BAWS configuration the fundamental 1064-nm radiation from the Nd:YAG (neodymium-doped yttrium-aluminum-garnet) laser is quadruped to 266 nm. Output at 266 nm is approximately 1 μJ per pulse with less than 1-nsec pulse width at a 10-kHz pulse rate. Note that BBO represents barium borate, Cr:YAG represents chromium-doped YAG, and KTP represents titanate phosphate.

The upper two histograms in Figure 8 are for two bacteria used as simulants for bioagents: *Bacillus globigii*, which is a simulant for *Bacillus anthracis* (anthrax), and *Erwinia herbicola*, which is a simulant for *Yersinia pestis* (plague). The lower left histogram shows a natural background measurement made in a desert environment at Dugway, Utah. The lower right histogram shows a ragweed pollen.

We see from Figure 8 that the bioagent-simulant histograms fall in the upper half of the plots and the

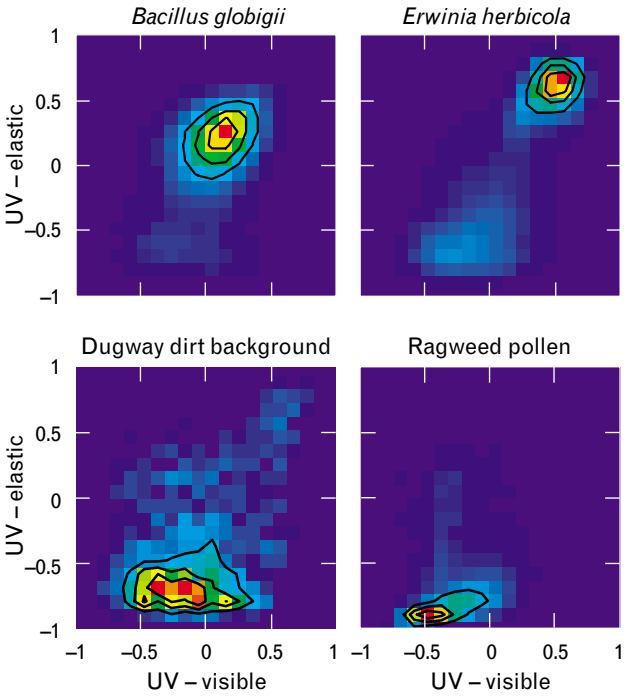

FIGURE 8. Histograms of detection events for the BAWS. Histograms are given as functions of the normalized difference between the ultraviolet (UV) and visible channels (horizontal axis) and the normalized difference between the UV and elastic channels (vertical axis). Histograms are shown for *Bacillus globigii* (a simulant for *Bacillus anthracis*), for *Erwinia herbicola* (a simulant for vegetative bacterial bioagents, such as *Yersinia pestis*), for ragweed pollen, and for a typical Dugway, Utah, dirt background. Note that bacteria can easily be distinguished from background dirt and pollen because of the separation on the histogram plots.

background histograms fall in the lower half of the plots. The simulant and background histograms are clearly separated. These features are common to other bioagent simulants (and actual bioagents) and other backgrounds. This separation in features allows us to discriminate threat particles from nonthreat particles.

The full real-time bioagent discrimination algorithm has been developed by Nathan R. Newbury at Lincoln Laboratory. It is, of course, more complicated than simply looking at the histograms, and we will not describe it here in mathematical detail. The following discussion, however, provides a general outline of how the sensor functions.

The BAWS operates continuously, storing measurements from every particle on which there are signals in all three channels. When the sensor is first turned on, it spends several minutes "learning" the background. The sensor then looks for "events," that is, significant changes from the background. If no events are detected, it continues to update the background. If an event is declared, the sensor classifies the event as threat or nonthreat. If the event persists long enough (e.g., fifteen seconds or more), an alarm is issued. The detection, classification, and alarm functions are all built into the BAWS and are completely automatic.

As illustrated in Figure 9, three generations of BAWS fluorescence sensors have been designed and

(a) (b) (c)

FIGURE 9. Three generations of the biological-agent warning sensor (BAWS). (a) The 1996 proof-of-concept sensor required a small van full of electronics for operation. (b) The 1997 BAWS II is a 3.4-ft^3 stand-alone sensor weighing 96 lb. (c) The 1999 BAWS III, carried by Thomas H. Jeys of Lincoln Laboratory, is less than 0.8 ft^3 and weighs about 19 lb. Detection and discrimination performance has improved with each generation.

FIGURE 10. Two BAWS IIIs at Dugway Proving Grounds, Utah, in the spring of 1999.

built. Gregory S. Rowe was the chief electronics and software engineer for all three designs. Robert P. Brady was the chief mechanical engineer for the latter two designs, which required considerable attention to packaging. In 1996 a proof-of-concept sensor was designed, fabricated, and field-tested at a major Government-run trial in only seven months. The sensor had a reasonably compact sensor head, but the electronics were commercial units housed in a mini-van. The prototype sensor had only the two fluorescence channels; it did not have an elastic-scattering channel. The sensor performed very well in the Joint Field Trials (JFT-3) conducted at Dugway Proving Grounds in Dugway, Utah, in the fall of 1996.

Following the success of the prototype sensor we designed a compact, self-contained BAWS, fabricated three sensors, and fielded them at Dugway for the JFT-4 trials in the fall of 1997. This BAWS II measures 3.4 ft^3, weighs 96 lb, and consumes 50 W of power. It can run on batteries as an autonomous unit, perform detection and discrimination functions with embedded electronics, and issue an alarm. The sensor was first implemented with only two channels; later an elastic-scattering channel was retrofitted.

During 1998 and 1999 we developed the BAWS III. This sensor has a redesigned optical head for increased sensitivity and new discrimination algorithms for improved performance. The BAWS III is less than 0.8 ft^3, weighs only 19 lb, and consumes only 40 W. Thus, the BAWS III is truly a portable sensor. The BAWS III was successfully tested in the spring of 1999. A photograph of two BAWS IIIs at Dugway Proving Grounds is shown in Figure 10.

The JFT-4 trials, held at Dugway Proving Grounds from 6 October to 2 November 1997, provided an independently refereed test of the BAWS II, along with other candidate early-warning sensors. Figure 11 shows an outline of the test arrangement. The test site comprised five test stations equally spaced along a 52-m line. At each test station, independent U.S.

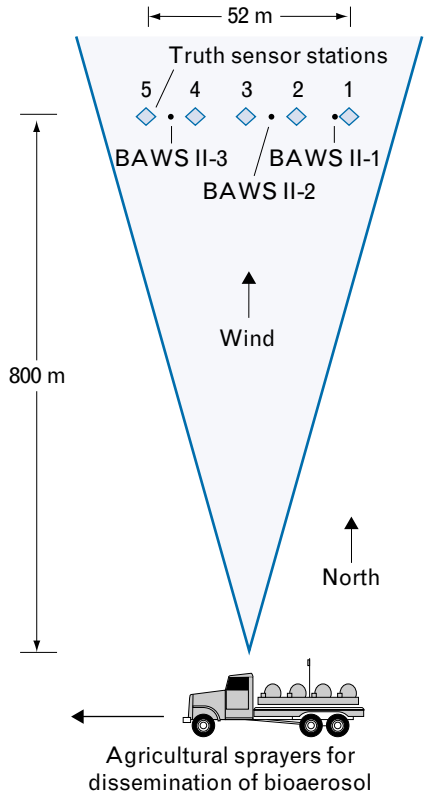

FIGURE 11. Test arrangement for the 1997 Joint Field Trials (JFT-4) at Dugway Proving Grounds. Harmless bacteria were dispensed upwind of the test grid by agricultural sprayers. Various sensors were stationed in the test grid, including three BAWS IIs, as indicated.

FIGURE 12. The bacteria dissemination truck for the Dugway trials. Harmless bacteria were dispensed from the agricultural sprayers on this truck. Note, however, that similarly unsophisticated equipment could be used to dispense real bioagents.

Army personnel operated conventional, slit-to-agar samplers to acquire so-called "truth" data. Following the tests, the agar plates were cultured and the bacterial colonies counted. Finally, some months after the trials the truth data were made available to us and to other test participants.

Participating test sensors were placed on either side of the test stations for official scoring. Our scored sensor was beside test station 1. We had two other sensors on the test site, but these were midway between test stations. They provided us with additional data but were not officially scored.

During the trials bacterial simulants were generated by agricultural sprayers mounted in the truck shown in Figure 12. The simulants were dispensed approximately 800 m upwind of the test stations and drifted across the site. Exact release times were not announced. The various early-warning sensors were required to issue alarm-on and alarm-off times. During JFT-4, 23 trials were conducted, 20 with *Bacillus globigii* and 3 with *Erwina herbicola*.

Figure 13 shows our scored BAWS II at the JFT-4 trials. The sensor is mounted on a tripod and has a vertical 2-ft air-sampling tube, so that the air intake is at the same height as the truth sensors. The slit-to-agar truth sensors are in the box to the left of the BAWS II; the box cover is removed during tests. To the right of the BAWS II is a simple particle counter that counts all particles—biological and nonbiological—in the 1-to-10-μm size range

The Dugway test site, shown in Figures 12 and 13, is a large, flat, high-desert environment, at a 4000-ft elevation, with low vegetation (less than 2 ft). As one might expect, such an environment has rather benign natural background conditions.

Figure 14 shows comparisons of the three BAWS II signals and the truth data for a representative *Bacillus globigii* release. The truth data are given in blue; they show that the simulated attack lasted about seven minutes and reached a level of about 50 particles per liter. (In the biological defense community the bioagent concentrations are normally expressed as agent-containing particles per liter of air [ACPLA].) This attack is a fairly modest one: if it had been an anthrax attack, a canonical unprotected person breathing normally would have not quite gotten a lethal dose.

The real-time signals from the BAWS II sensors are shown in red. We see that they agree very well with the truth data. The shaded area shows when BAWS II-1 (the officially scored sensor) was in alarm. We see that the BAWS II went into alarm when the particle concentration was only about 2 ACPLA. We also

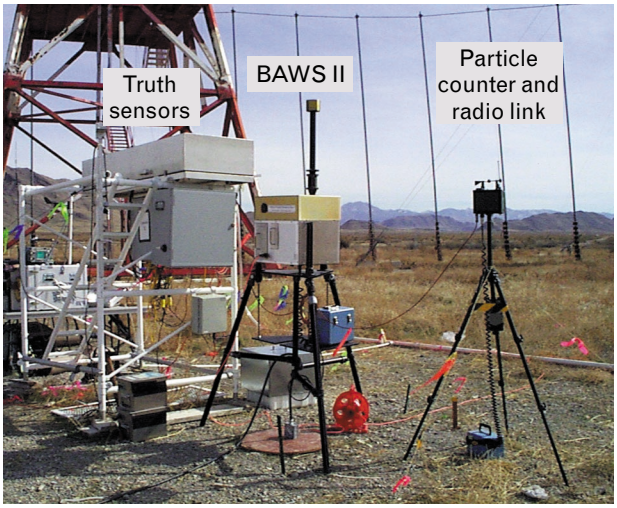

FIGURE 13. BAWS II mounted on a tripod at Dugway Proving Grounds. The BAWS II is a self-contained, stand-alone unit powered by batteries in the blue box. Air is drawn in through the tube on top, which was extended above the sensor to be at the same height as the truth sensors. To the left of the BAWS II are the truth sensors—rotating slit-to-agar culture plates. To the right of the BAWS II are a simple particle counter and the radio link for the BAWS II alarm signal.

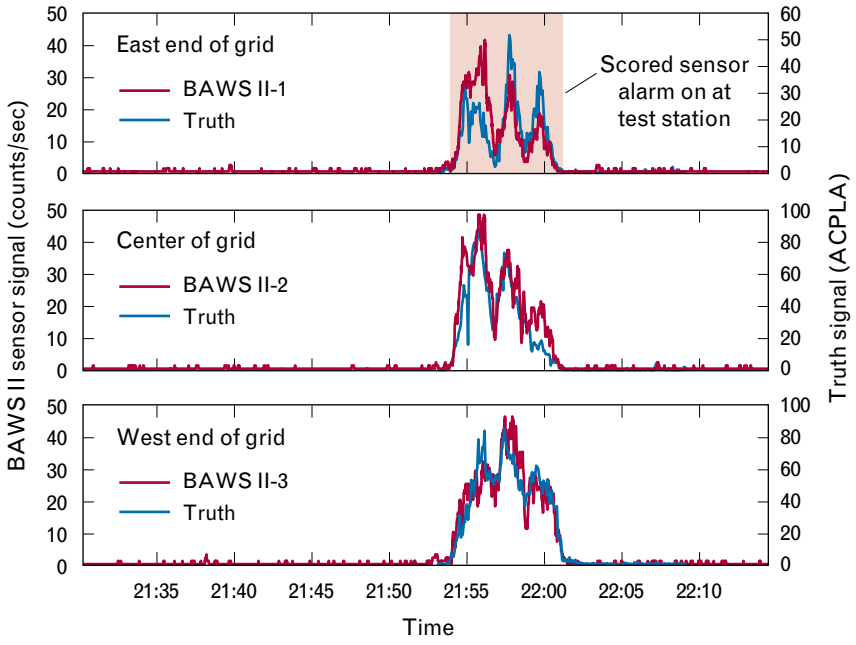

FIGURE 14. BAWS II and truth signals as a function of time for a *Bacillus globigii* release. Note the excellent agreement between the real-time BAWS II signal and the truth signal obtained after several days of culturing the collected bacteria. The BAWS II correctly issued an alarm at a particle concentration of less than five agent-containing particles per liter of air (ACPLA). Note also that although the three BAWS IIs generally measure the same concentrations, there are significant variations in the cloud concentrations even though the sensors are only fifteen to twenty meters apart.

note that there can be considerable differences in particle concentrations measured by the three BAWS IIs, even though the sensors were only spaced about fifteen to twenty meters apart.

In Figure 15 we show a trial that demonstrates the ability of BAWS II to discriminate a bioagent-simulant cloud from a dirt cloud. We again plot the truth data in blue and the BAWS II signal in red. Now we also plot, in green, the data from the simple particle counter. In this trial, before the release of *Bacillus globigii*, there were trucks driving around the site stirring up large clouds of dirt. As we see from Figure 15 there are six dirt events, two of them higher than 1000 particles per liter. The BAWS II did not trigger an alarm on any of these events; its discrimination algorithm identified each of them as a dirt event. The BAWS II did, however, correctly trigger an alarm on two simulant events, even though the total numbers of particles for these events were much less than for the dirt events. As seen in the expanded view of Figure 15, the maximum concentration for one of the simulant clouds was less than 20 ACPLA.

The BAWS II performed extraordinarily well at JFT-4. The scored sensor showed a sensitivity of about 5 particles/liter and had a response time of 26 sec. It correctly declared alarms on all the most stressing trials (defined officially as less than 15 ACPLA) and correctly declared alarms on all but one of the less-stressing trials (above 15 ACPLA). (The one missed trial seems to have resulted from a software glitch; the release was actually one of the larger ones, and we easily triggered an alarm when we played the recorded raw data back through the real-time algorithm after the trials.) The BAWS II had no false alarms. In addition, the sensor was able to discriminate the bioagent simulants from unintentional inteferents, such as dirt clouds and diesel fumes.

The BAWS II also proved robust in the field environment. The three sensors operated for 170 hours each during the test period. They operated autonomously, under battery power. They even survived driving rain and snow.

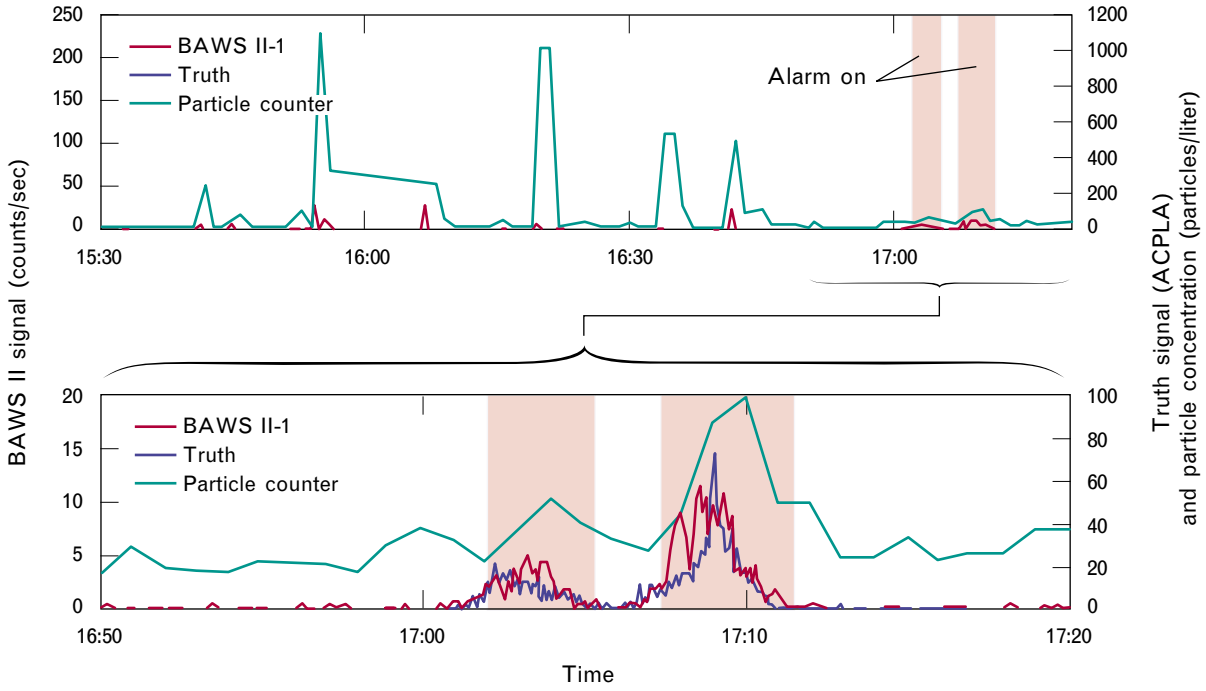

FIGURE 15. BAWS II, truth, and particle-counter signals as a function of time for a *Bacillus globigii* release in the presence of dirt clouds. The upper plot shows a roughly two-hour time period during which vehicles were stirring up dirt. The latter part of the upper plot and the expanded lower plot show the actual simulant cloud. Note that the BAWS II did not trigger an alarm on dirt clouds of about 1000 particles/liter but correctly triggered an alarm on a biological cloud at a level of less than 10 particles/liter.

Laser Induced Fluorescence for Stand-Off Detection

The BAWS laser-induced-fluorescence sensor is a local (or point) sensor: it detects only those particles that actually flow through the sensor. On the other hand, the BAWS can be regarded as an extremely short-range lidar, where the distance from the laser transmitter to the sensed bioparticles is only a few centimeters.

In principle, laser-induced fluorescence can be used to make a much longer-range biodetection lidar system. The U.S. Army is developing the Short-Range Biological Standoff Detection System (SR-BSDS) to explore this possibility [15]. Shen Shey, Robert Kramer, and Michael O'Brien at Lincoln Laboratory have analyzed the performance and potential of the SR-BSDS.

Compared to the BAWS point sensor there are many technical challenges in building a standoff laser-induced fluorescence lidar. Obviously, the UV laser and the transmitter/receiver optics must both be much larger to achieve long-range capabilities. Furthermore, some fundamental physics effects severely limit the performance of a UV lidar. Chief among these is that UV light is strongly absorbed (principally by ozone) and scattered in the atmosphere. For example, with a 266-nm laser, the signal in the UV fluorescence channel would, under moderately good atmospheric conditions, be reduced by a factor of 10^4 in going from a range of 1 km to 5 km.

To somewhat overcome the limitations of atmospheric absorption and scattering, we can have the lidar system look over a wide range gate to increase the number of bioparticles it senses on a given laser pulse. Unfortunately, sensing in a wide range gate makes the discrimination of threat particles from the background more difficult, since the detected signal comes from a mixture of many potentially different kinds of particles. For the BAWS, one of the factors that makes discrimination possible is that the aerosol particles are individually sensed.

Even with wide range gates, our analysis shows that the ranges achievable from a UV lidar system will

only be a few kilometers and that the concentrations detectable at these ranges will be large. It appears that the best way to use a UV lidar would be to interrogate a bioagent cloud at the release point (e.g., at the impact point of an enemy missile), where the concentrations are high (perhaps 10^5 to 10^6 particles/liter). Under this operational concept a reasonably sized UV lidar system might be able to detect a bioagent release out to five kilometers.

We presume that people support detecting and discriminating a bioagent cloud and issuing a warning before the cloud reaches them. Thus, even with its relatively short range, a standoff lidar could be useful in an overall detection and warning system; we showed such a lidar in the military-port defense architecture in Figure 2. We observe, as an example, that if the wind speed were 20 km/hour (10 kt), and if the lidar were able to detect a release 2 km upwind, it would provide the port or air base with an additional six minutes of warning time.

Background Measurements

The BAWS described earlier can detect single bioaerosol particles. Likewise, the bioelectronic sensor to be described in the next sections can, in principle, identify a substance from a single-particle sample. Thus, these sensors have extraordinary sensitivity, given a pure sample. Consequently, the ultimate performance of these sensors will not be limited by their fundamental sensitivities, but by the effects of background particles in the sample volume.

Although we often do not perceive them, the air we breathe is heavily laden with a wide variety of aerosol particles. (See the sidebar entitled "The Natural Aerosol Background.") There are ordinary dust and dirt particles. There are natural bioaerosols, such as pollen, mold spores, and benign bacteria. There are anthropogenic particles, such as particles in diesel exhaust and particles from automobile tires. The total number of background aerosol particles per liter of air normally exceeds the desired sensitivity of a bioagent sensor by many orders of magnitude.

Background aerosols can have two significant deleterious effects on a bioagent sensor. First, they can mask real biological attacks, causing a sensor to miss an attack. Such a missed detection could, of course, be catastrophic. Second, the background aerosols can erroneously trigger the bioagent sensor, causing a false alarm. A false alarm is not catastrophic; but if false alarms are too frequent, people will quickly begin to ignore the alarms, and the sensors will become useless.

Thus, to develop a practical bioagent detector, we must understand the aerosol background. Further, we must understand how the background affects the detection probability and false-alarm rate of a bioagent detector.

Many measurements have been made and continue to be made of the atmospheric aerosol background. For instance, the aerobiology community regularly monitors the concentrations of pollen and mold spores in the air. As another example, the Environmental Protection Agency (EPA) monitors the total number of particles in several size ranges. Unfortunately, existing background measurements are inadequate for our purposes because of two major deficiencies.

First, existing measurements do not have adequate time resolution. Pollen counts, for instance, may only be measured and reported on a daily basis. Other measurements may be made on an hourly basis. In contrast, as can be seen from Figures 14 and 15, bioagent attacks typically occur on relatively short time scales. As a biological-agent cloud drifts over a site it may have a rise time of less than a minute. It may remain over a site for about ten minutes and then drift away in less than one minute. Thus, the time scales we care about for a biological attack are typically in the range of ten seconds to ten minutes.

Second, existing background measurements do not use techniques representative of those we expect to use for bioagent detectors. In particular, existing measurements do not use fluorescence detection. We care about the background, after all, only insofar as it affects our measurements. For instance, there may be many background aerosols that are sensed by a total particle counter but that do not fluoresce. These particles would be totally unimportant to our BAWS fluorescence sensor.

To obtain relevant data on background aerosols Lincoln Laboratory, under the direction of Nathan R. Newbury and Jae H. Kyung, is conducting a back-

THE NATURAL AEROSOL BACKGROUND

UNFILTERED AMBIENT air customarily teems with tiny aerosol particles. Except under extreme conditions (e.g., a dust storm), we do not normally sense these particles; although almost everyone has seen floating dust motes illuminated by a sun beam, and persons afflicted by hay fever sense pollen grains in the air even if they can not see them. It is in the presence of this natural aerosol background that bioagents must be sensed.

The situation is illustrated in Figure A. We would like to detect bioagent particles at concentrations as low as 1 particle per liter of air. In a liter of air in a remote, semiarid environment, however, there may be several hundred to a thousand other aerosols in the size range of a bioagent particle (1 to 10 μm). In a liter of urban air there may be 10,000 such particles.

Figure B gives more quantitative information on the natural background. We plot the number of particles above a given diameter against particle diameter for four representative conditions [1]. Note that these are nominal, average conditions; particle concentrations may easily fluctuate an order of magnitude around these conditions.

We see from Figure B that the particle concentration is a strong function of particle size. There are typically millions of particles above 0.1 μm, thousands of particles above 1 μm, and only a few particles above 10 μm. This strong size dependence occurs because large particles rapidly fall out of the air, whereas small particles are buoyant enough to stay airborne for long periods of time.

We also see from Figure B that there are significant differences in the particle concentrations in different environments. In the 1-to-10-μm size range the remote, semiarid environment has the fewest background particles; the urban environment has the most; and the rural environment falls in between.

In addition to differing numbers of particles, the different environments have different compositions of aerosol particles. In arid and semiarid environments most of the natural aerosol particles are soil derived—mainly clay minerals such as illite, mixed-layer clays, and kaolinite [2].

Rural environments add biological aerosols to the soil-derived background. There are many different types of biological aerosols, including fungal spores, bacteria, pollen, plant spores, plant debris, algae, protozoa, insect parts and feces, skin cells, and viruses [3].

In urban environments anthro-

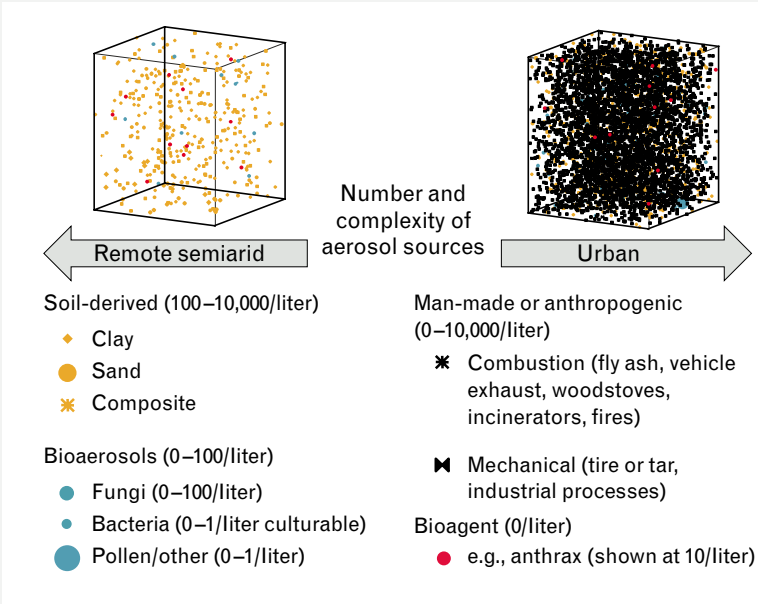

FIGURE A. Illustrations of the number and composition of background aerosol particles in the air. Concentrations of particles 1 to 10 μm in diameter range from a few hundred per liter in remote semiarid environments to greater than 10,000 particles per liter in urban environments.

genic aerosol particles are added to biological and soil-derived particles. Anthropogenic particles come from coal and oil-burning plants, diesel and gasoline engine exhaust, road-dust resuspension and tire-particle generation from vehicle movement, wood-burning stoves, and industrial processes [4].

Soil-derived aerosol particles are generally not a significant interferent for UV fluorescence-based sensors. They can, however, be a major problem for simple particle counters, and they can clog or otherwise overwhelm identifying sensors.

Of the biological aerosols, fungal spores are by far the most important interferents for a bioagent sensor. Fungal spores are ubiquitous: wherever there is decaying organic matter, there are fungal spores. They are about the same size as bioagent particles. They are viable biological particles, so they contain many of the same basic biological components as bioagents. Finally, concentrations of 10 particles/liter are common, and concentrations can easily reach greater than 100 particles/liter.

Natural bacteria are not particularly important interferents for two reasons. First, concentrations are usually lower than 1 particle/liter. Second, natural bacteria normally are found rafting on larger airborne particles.

Although it might be hard to believe for those who suffer from hay fever, pollen is an insignificant interferent for bioagent sensors. Pollen grains are large—20 to 100 μm; they are, in fact, this large so that they will readily fall out of the air onto plants to perform their pollination function. Thus, airborne concentrations of pollen are very low; even during peak pollen seasons average concentrations rarely exceed 1 particle/liter. For those unusual occasions when the pollen concentration exceeds 1 particle/liter (e.g., directly under an oak tree in May), the pollen grains may easily be distinguished from bioagent particles on the basis of their size.

For a UV fluorescence-based bioagent sensor, the most important anthropogenic particles are polycylic aromatic hydrocarbons (PAHs) generated in incomplete combustion of fossil fuels. PAHs fluorescence strongly under UV light; thus, if enough PAH molecules are adsorbed on a particle of the right size, the signature might mimic that of a bioagent particle. Other anthropogenic particles may spoof particle counters or clog identifying sensors.

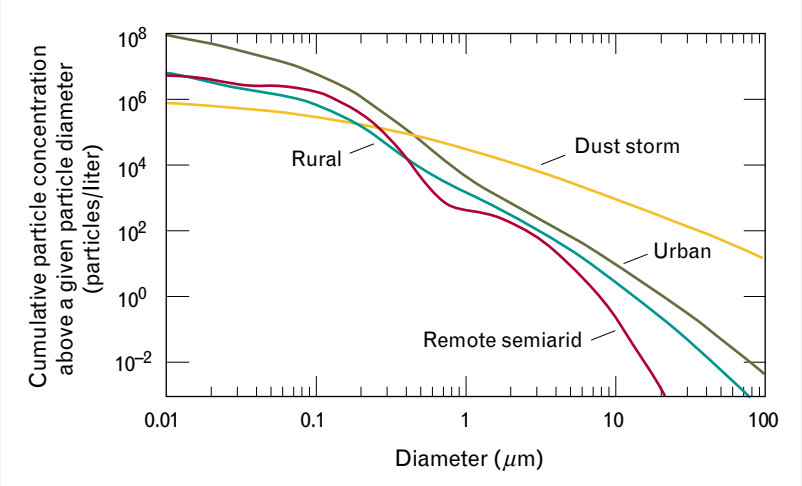

FIGURE B. Representative cumulative concentration of particles above a specified particle diameter. The concentrations vary significantly from location to location. For all locations the concentrations decrease sharply as the particle diameter increases.

References

1. R. Jaenicke, "Tropospheric Aerosols," in *Aerosol–Cloud–Climate Interactions,* P.V. Hobbs, ed. (Academic Press, San Diego, 1993), pp. 1–31.
2. E.M. Patterson, "Size Distribution, Concentrations, and Composition of Continental and Marine Aerosols," in *Atmospheric Aerosols: Their Formation, Optical Properties, and Effects,* A. Deepak, ed. (Spectrum Press, Hampton, Va., 1982), pp. 1–38.
3. H.A. Burge, ed., *Bioaerosols* (Lewis Publishers, Boca Raton, Fla., 1995); C.S. Cox and C.M. Wathes, *Bioaerosols Handbook* (Lewis Publishers, Boca Raton, Fla., 1995).
4. J.M Prospero, R.J. Charlson, V. Mohnen, R. Jaenicke, A.C. Delany, J. Moyers, W. Zoller, and K. Rahn, "The Atmospheric Aerosol System: An Overview," *Rev. Geophys. & Space Phys.* **21** (7), 1983, 1607–1629; R.M. Harrison and R.E. van Grieken, *Atmospheric Particles* (Wiley, New York, 1998).

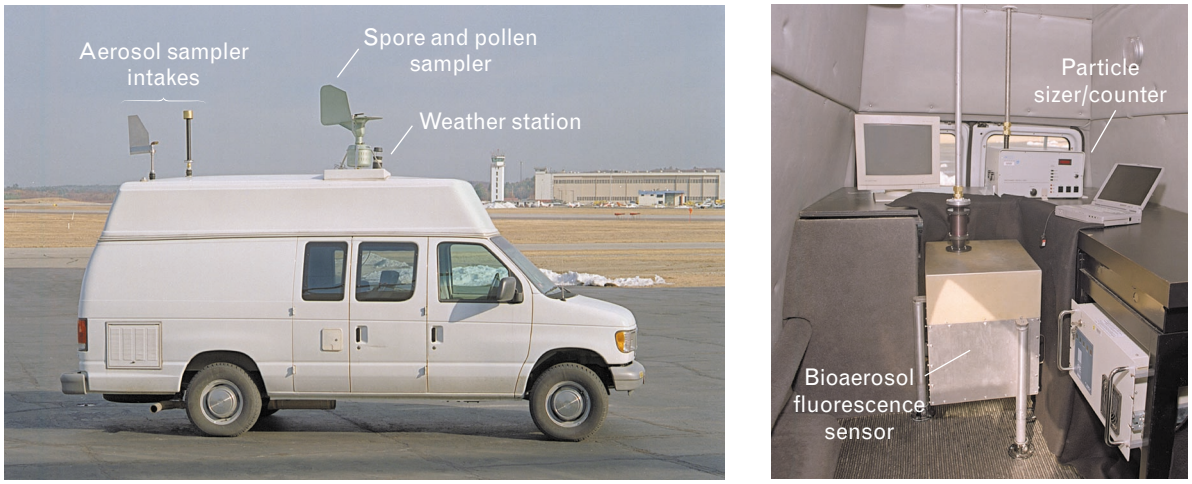

FIGURE 16. The Lincoln Laboratory mobile bioaerosol laboratory. This van contains a BAWS sensor as well as several commercial sensors, including a particle sizer/counter, a spore and pollen sampler, and a slit-to-agar sampler. Measurements can be made with the van either stationary or moving.

ground measurement program. We have equipped a van, shown in Figure 16, with various instruments. The principal instrument is a BAWS fluorescence sensor. We have also purchased and installed various commercial instruments including a TSI aerodynamic particle sizer to measure the total number of particles as a function of size, several slit-to-agar samplers to measure culturable bioaerosols, and a Burkard spore/pollen sampler to collect large aerosols on tape for later counting under a microscope. In addition, we have included routine meteorological instrumentation to measure wind speed and direction, air temperature, and relative humidity.

Figure 17 shows sites from our extensive measurement campaign in progress throughout the continental United States. Data have been taken in urban, desert, rural, and coastal areas. Generally, data are taken continuously for a week at each location. We have returned to some locations during different times of the year to assess seasonal variations. Measurements are planned for additional locations in the United States and abroad.

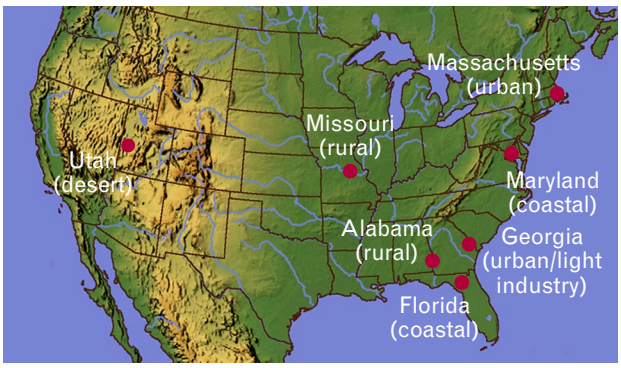

FIGURE 17. Locations where background measurements have been made. Measurements have been made across the country in urban, rural, and desert sites.

Figure 18 shows background data analyzed and compiled by Ann E. Rundell. The data are from five different locations representing desert, urban, rural, and coastal environments. We plot the power spectral density of the aerosol particle concentrations measured by the BAWS. For this plot a counted particle is one that had a signal in all BAWS channels; the discrimination algorithms discussed in connection with Figure 8 have not yet been applied.

We draw a number of interesting conclusions from Figure 18. First, we observe that there is wide variation in the backgrounds at the five different sites. The urban and rural sites in Alabama, Georgia, and Missouri have the highest background fluctuations; the coastal and desert locations in Maryland and Utah have the lowest.

We also see from Figure 18 that the background fluctuations decrease significantly as a function of frequency. The fluctuations in the region that we care about (from ten seconds to ten minutes) are much less than those at longer time scales. This phenomenon is further illustrated in Figure 19, in which we

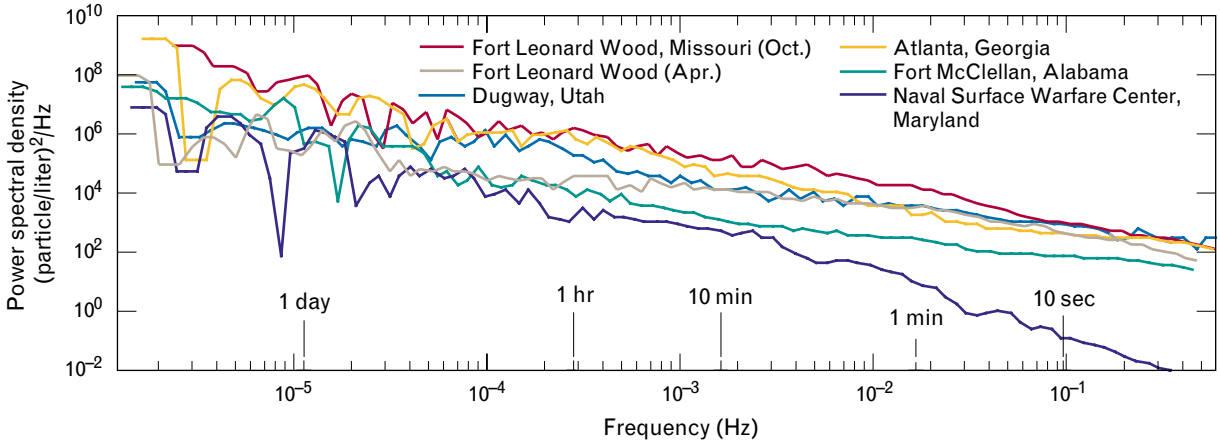

FIGURE 18. Power spectral density of aerosol particle fluctuations measured by the BAWS at various sites. Each plot is from one week of continuous measurements. Each plot has roughly an inverse frequency ($1/f$) dependence, but there are significant differences in magnitude from site to site.

plot a time history of particles per liter measured by two different sensors. The green curve shows the fungal spore count as measured by the Burkard spore trap. The red curve shows particles measured by the BAWS sensor as having fluorescence signatures in the region expected for mold spores. We see that the two sensors agree well on the general fluctuations in fungal spores. More importantly, we see that most of the fluctuations are on a diurnal basis. These long-time-scale variations are easily distinguishable from those expected during a biological attack.

Another feature apparent from Figure 18 is that the fluctuations decrease with approximately an inverse frequency ($1/f$) dependence. A $1/f$ dependence is characteristic of noise spectra that are driven by many different distinct events [16]. Indeed, we find that we can correlate many of the largest background fluctuations with discrete, principally man-made events. Figure 20 illustrates this effect. The upper plot shows a temporal history of fluorescent particles per liter for Friday, 9 October 1998, when there was considerable human activity at Fort Leonard Wood, Missouri. The activities included trucks and backhoes moving around, and even the detonation of an explosive. The plot identifies approximately when these activities occurred. We see that there are large, short-time-scale increases in the background associated with these activities; the exact times do not overlap because the activities were at various distances from the sensor, and it took time for the aerosols kicked up into the air to drift past the sensor.

The lower plot in Figure 20 shows measurements of the same site on Sunday, 11 October 1998, during the long Columbus Day weekend when there was little human activity around the site. We see that the fluctuations are very much lower than those in the upper plot.

As we mentioned earlier in this section, the important aspect of the background is how it affects a

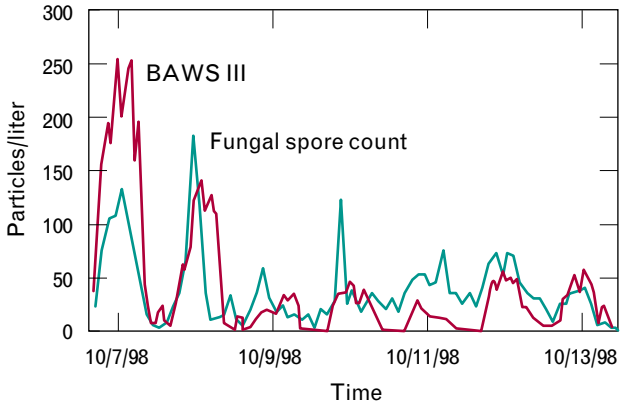

FIGURE 19. Concentrations of fungal spores versus time at Fort Leonard Wood, Missouri. The green curve gives fungal spores that were collected by a Burkard spore trap and manually counted under a microscope. The red curve gives the particles measured by a BAWS specifically tuned to detect fungal spores. Note the generally good agreement between the two sensing techniques.

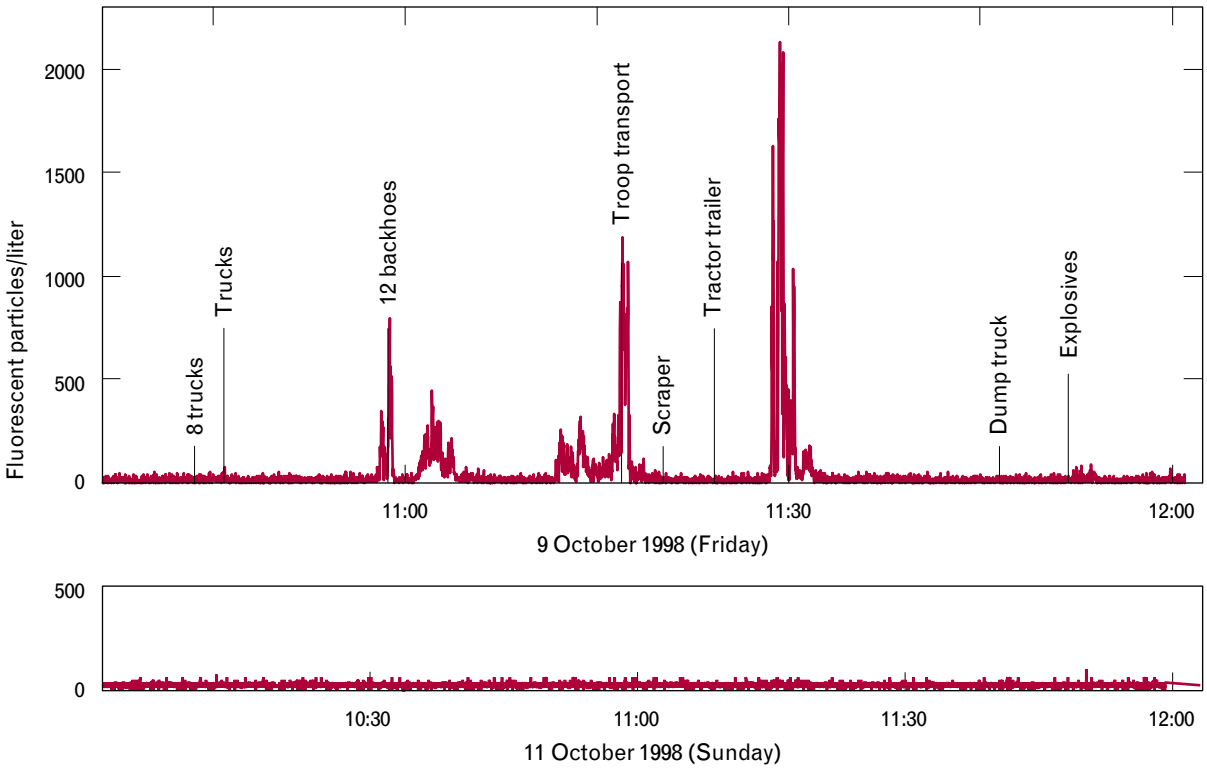

FIGURE 20. Background measurements with the BAWS at Fort Leonard Wood, showing the variability with human activity. The upper plot from 9 October 1998 (Friday) shows large fluctuations resulting from various activities near the sensor. The lower plot from 11 October 1998 (the Sunday of the Columbus Day weekend) shows a low, flat background in the absence of human activity at the site.

sensor's detection probability and false-alarm rate. In real field trials at Dugway Proving Grounds we found that the BAWS sensor had essentially perfect detection with no false alarms; but Dugway Proving Grounds is a desert site, with rather benign background, and human activity is restricted during tests. We do not have the capability to release bioagent simulants at the other sites where we conducted background measurements, but we can combine the background measurements with the Dugway trial data to simulate sensor performance at sites with more stressing background conditions.

Figure 21 shows performance curves generated by Nathan R. Newbury by combining background data with Dugway trial data to simulate a 120-particle/liter anthrax attack. We plot probability of detection versus false-alarm rate for desert, rural, and urban sites. These calculations were done for a fairly simple detection and discrimination algorithm, as implemented in the BAWS three-channel sensor. We see

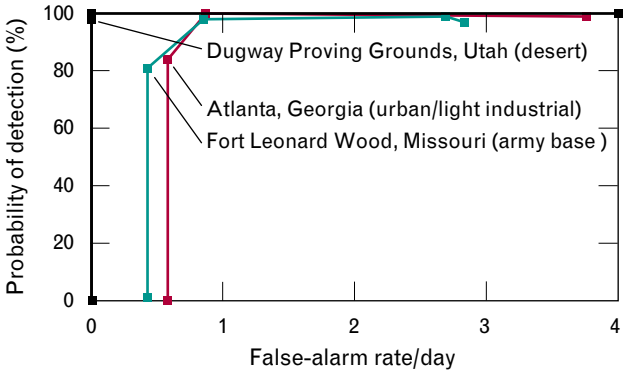

FIGURE 21. Probability of detection versus false-alarm rate calculated for the BAWS III for three different locations. A *Bacillus anthracis* attack at a concentration of 120 particles/liter is assumed. The curves were generated by using measured *Bacillus globigii* releases at Dugway Proving Grounds and background measurements at each of the sites. Performance is perfect at the Dugway site (100% detection, no false alarms) and excellent at the other sites (100% detection at less than one false alarm per day). With more background data collection and more sophisticated alarm algorithms the false-alarm rate can be further improved.

that, consistent with the Dugway trial data, performance is perfect at the desert site—100% detection with zero false alarms. At the urban and rural sites, performance is somewhat worse but still good: we get 100% detection with a false-alarm rate of less than one per day at the urban Atlanta and rural Fort Leonard Wood sites.

With increased background data collection and further refinements in the alarm algorithm we expect to decrease the false-alarm rate for the BAWS sensor to less than one per week with essentially 100% detection, in even the most stressing background conditions.

Bioelectronic Identifying Sensor

The BAWS fluorescence sensor is an early-warning sensor: it rapidly detects and discriminates threat aerosol particles, but is does not identify the bioagent. Thus, there is need for a downstream identifying sensor. This sensor would be dormant until triggered by the continuously operating BAWS. It would then precisely identify the bioagent to confirm the attack and guide medical response.

Todd H. Rider at Lincoln Laboratory invented a bioelectronic identifying sensor that combines living cells with microelectronics [17]. The genesis of this sensor was his observation that white blood cells, which detect pathogens within human (and other animal) bodies, respond more rapidly, sensitively, and specifically than currently available man-made sensors. This observation led to the approach of using white blood cells as the basic sensing elements and interpreting them with an optoelectronic system to provide rapid signal readout.

We use a type of white blood cell known as a B lymphocyte; these B cells can be harvested from mice and then grown for many years in an artificial environment, given the appropriate culture medium and ambient conditions. B cells have the property that their surfaces are covered with antibodies. In nature, these surface antibodies detect a pathogen by binding to its antigens (surface features); this binding then triggers biochemical reactions in the B cell. It is this natural antibody/antigen binding and biochemical-reaction sequence that we make use of in our B-cell sensor.

The B-cell sensor requires two critical pieces of genetic engineering to make it into a bioagent identifier. First, we engineer the B cells so they have antibodies that are specific to certain bioagents. Second, we add the aequorin gene to the B cells. Aequorin is a bioluminescent protein found in a species of glowing jellyfish. Adding it to the B cells makes them glow when they detect a bioagent. This work is done in conjunction with Jianzhu Chen of MIT.

Figure 22 illustrates the basic operation of the B-cell sensor. The genetically engineered B cells are attached to a transparent substrate; behind the substrate is a CCD array. A liquid sample containing possible bioagents is injected into the cell culture liquid surrounding the B cells. If a bioagent particle with the proper antigen drifts by, it binds to the surface antibodies on the B cell. Binding of the bioagent to the B cell's antibodies triggers a cascade of biochemical reactions within the B cell. This cascade amplifies the single binding event and results in the release of many Ca^{2+} ions in the B cells. The Ca^{2+} ions then induce the aequorin to emit photons. Thus, a B cell that detects a bioagent will emit light. This light

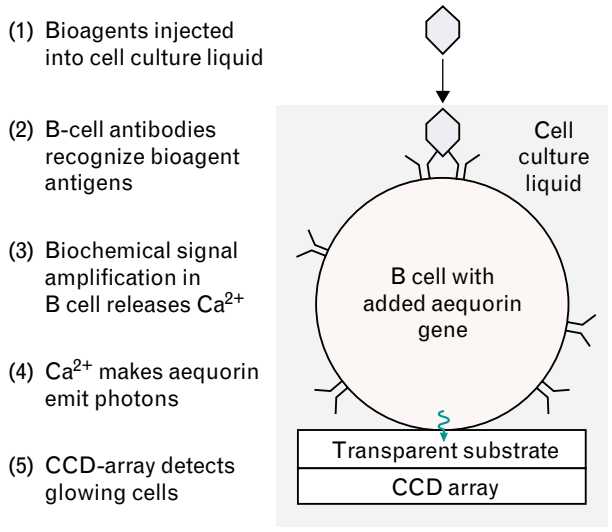

FIGURE 22. Principles of a bioelectronic identifying sensor using living B cells. B cells are genetically engineered so that their surface antibodies recognize bioagent antigens. The aequorin gene (which is what makes certain jellyfish glow) is also added to the B cells. When a bioagent antigen attaches itself to the engineered B cell, a biochemical amplification process results in the B cell emitting light. This light can then be detected by a CCD array.

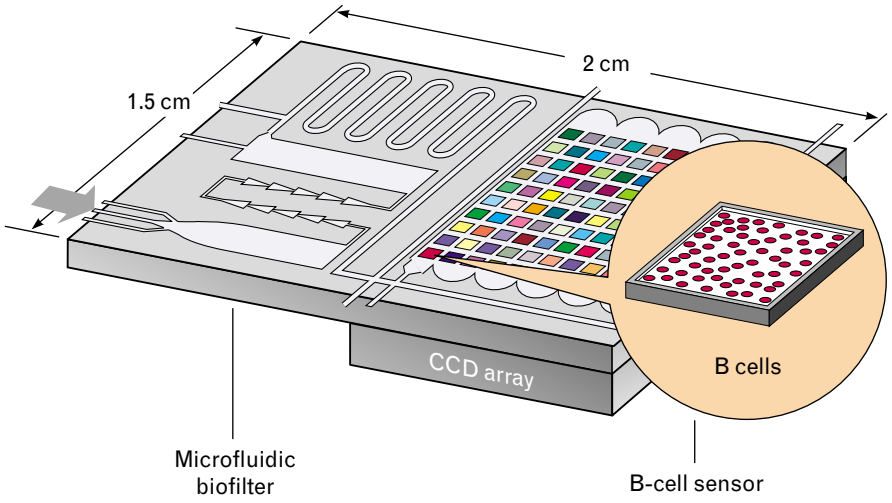

FIGURE 23. Schematic illustration of a bioelectronic identifying sensor. A microfluidic bioprocessor takes in a sample and purifies it for presentation to the measurement section. The measurement section comprises many patches of B cells, with the cells in each patch engineered to detect a particular bioagent. The bioagent is identified by observing which CCD element senses light output. Microfluidics in the measurement section brings nutrients to the B cells and carries waste products away.

can then be detected by an element of the CCD array. Finally, an electric output from the CCD array will signal a bioagent detection.

Our calculations indicate that a single bioagent particle detected by a single B cell should induce enough light to be detected by the CCD. Thus, the B-cell sensor is potentially a single-particle detector. It should be possible to engineer different B cells to detect the entire panoply of bioagents—bacteria, viruses, rickettsiae, fungi, and proteinaceous toxins.

An overview of a possible bioelectronic-sensor implementation is shown in Figure 23. There might be 100 patches of B cells over a 1-cm × 1-cm CCD array. Each 1-mm × 1-mm patch would contain thousands of B cells. Each patch could be engineered to respond to a particular bioagent. Thus, light on a particular area of the CCD array would precisely identify that a specific bioagent had been detected.

The compact structure shown in Figure 23 will depend in large measure on microfluidic technology. (See the sidebar entitled "Microfluidic Technology.") Microfluidics will be used to flow the liquid sample containing potential bioagents through the B-cell sensor. Microfluidics will also flow nutrients to the B cells to keep them alive and remove B-cell waste products. A microfluidic bioprocessor can be used to filter and purify the sample before it is sent to the B-cell sensor. This filter helps assure that the B-cell sensor does not get clogged with impurities.

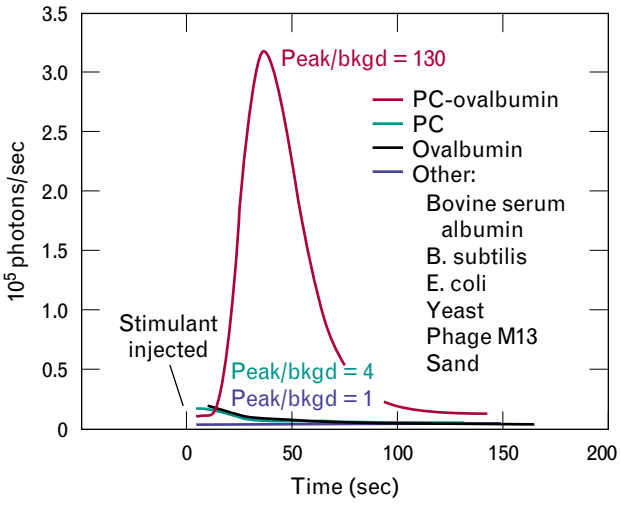

FIGURE 24. Measured response of B cells that were genetically engineered to respond to phosphorylcholine (PC)-ovalbumin. The red curve shows the large, rapid response when the B cells are exposed to the PC-ovalbumin. The other curves show the lack of response when the B cells are exposed to similar substances and to other possible interferents.

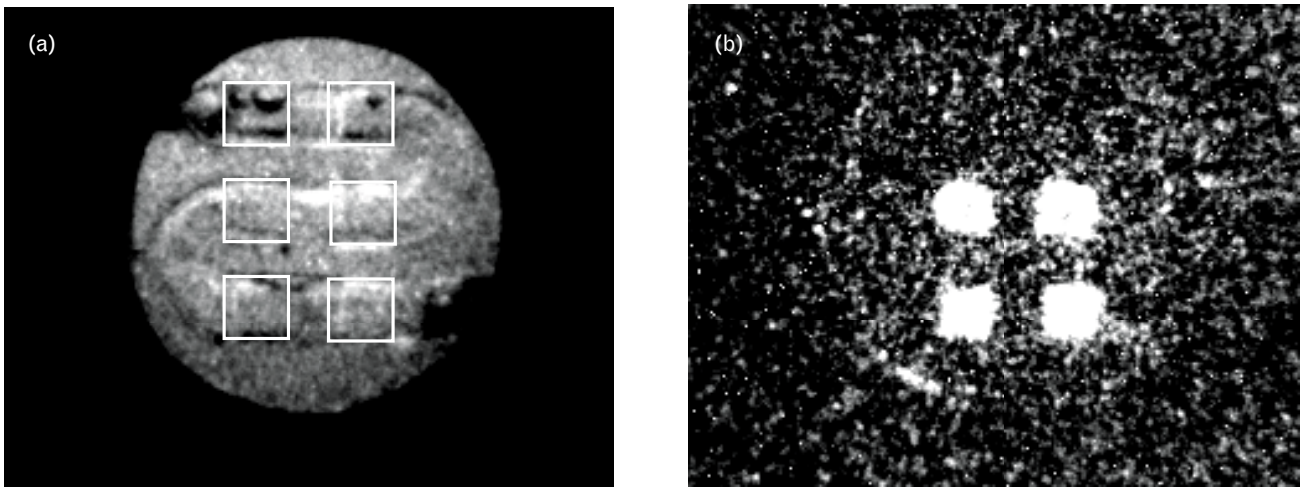

FIGURE 25. Microfluidic test chip for a bioelectronic B-cell sensor. (a) The microfluidic flow channel and six 2-mm × 2-mm cell sites along the flow channel. The lower four sites were loaded with a monolayer of B cells. (b) The four B-cell sites glowing brightly 20 sec after the appropriate simulant bioagent was injected.

The B-cell identifying sensor is in an early stage of development, but feasibility tests conducted thus far have been encouraging. We have performed tests to demonstrate both the rapid time response and the specificity of the basic B-cell reaction. We performed these tests with B cells that have antibodies specific for phosphorylcholine(PC)-ovalbumin, a nonpathogenic molecule. Martha S. Petrovick genetically engineered these cells by inserting the aequorin gene. We then tested the response of the engineered B cells by injecting them with PC-ovalbumin.

Results obtained by Rider are shown in Figure 24. We see that the response is very rapid: peak light output occurred in about thirty seconds. The measured light output was more than one hundred times the background level—an easily detectable signal.

To test the specificity of the B-cell detection process, we exposed the cells to various other substances. These results are also shown in Figure 24. There was very little response when the B cells were exposed to just PC or ovalbumin. There was no measurable response to bovine serum albumin, which is similar to ovalbumin. We also exposed the B cells to common contaminants that might be present in environmental samples: *Bacillus subtilus* (a common bacterium), *E. coli* (another common bacterium), yeast, M13 (a virus), and sand. There was no measurable response to any of these substances. We conclude that the B-cell reaction is highly specific to PC-ovalbumin.

We have also performed a proof-of-principle test of the planned sensor configuration illustrated earlier in Figure 23. Albert M. Young generated a six-site microfluidic test chip, as shown in Figure 25. Each cell site in the chip is a 2-mm × 2-mm glass surface within the microfluidic channel. In the test shown in Figure 25, four of the six cell sites were loaded with a monolayer of B cells engineered to respond to anti-IgM. Fluid containing anti-IgM was then flowed through the microfluidic test chip and the test chip was observed with a camera. Figure 25 shows that only twenty seconds after the fluid was injected, the four B-cell sites were glowing brightly.

Many questions remain to be answered before a practical B-cell identifying sensor can be fielded. For instance, can the patches of B cells be kept stable and isolated on the transparent substrate? Can the B cells be stored for extended periods before use? Can the B cells be kept alive long enough in deployed sensors? We are working to demonstrate positive answers to these questions and to develop alternative solutions in case some of the initial answers are negative. For instance, it appears from early tests that B cells can be made to stick well enough to glass substrates, but in case they do not Laura T. Bortolin came up with the idea of using fibroblast cells instead of B cells for the bioelectronic sensor [18]. All results to date show that

MICROFLUIDIC TECHNOLOGY

MICROFLUIDIC TECHNOLOGY, as implied by its name, is technology for producing integrated submillimeter fluidic networks for the transport, manipulation, and reaction of liquids. Microfluidics is perhaps best described in analogy to microelectronics. Microelectronics involves the integration of many electronic components—transistors, diodes, resistors, etc.—in compact, rugged, easily producible packages. Likewise, microfluidics involves the integration of many fluidic components—valves, pipes, mixing chambers, etc.—in compact rugged, easily producible packages. Microelectronic technology has produced a revolution in computer and communications technology and, concomitantly, revolutionary changes in people's lives. Microfluidics may not alter the world as dramatically as microelectronics has, but we expect that microfluidics will bring revolutionary changes to biochemical, biological, and medical processing fields.

For bioagent sensors, microfluidic structures offer three potential advantages over more conventional fluid handling. First, they are compact and rugged, making them ideal for field sensors. Second, they are inexpensive to manufacture; thus, they will not dominate overall sensor cost and, indeed, might be considered as disposable components in sensors. Finally, they enable measurements to be made with tiny amounts of fluids (perhaps nanoliters or even picoliters); a sensor this abstemious with consumables reduces routine maintenance requirements and overall life cycle costs.

Albert M. Young, Theodore M. Bloomstein, and others at Lincoln Laboratory have developed a novel microchemical etching process to produce microfluidic components [1]. This process is illustrated in Figure A. Silicon substrates are etched in a chlorine environment by focusing an argon-ion laser beam to locally melt the silicon. In this melting process silicon chlorides are formed; these rapidly diffuse from the surface, minimizing local particulate formation and leaving a clean etch. Computer control of the laser pointing and focus and of the silicon-substrate position allows us to produce precision three-dimensional laser-micromachined components.

Once the silicon substrate has been etched, it can be used as a master mold to replicate the microfluidic structure cheaply and accurately. Replica components have been generated in a three-stage process. First, we fluorinate

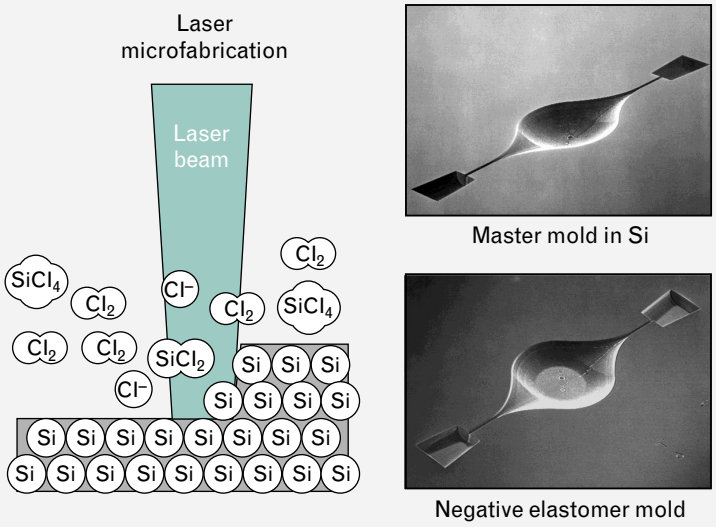

FIGURE A. Microfluidics fabrication process. Submicron structures are formed in silicon by using chlorine-assisted laser etching. The silicon piece serves as a master mold from which a negative elastomer mold is generated. Finally, inexpensive polymer replicas of the originally silicon structure are formed from the negative elastomer mold.

the silicon (with tridecafluoroctaltrichlorosilane). Next, we generate a negative mold by casting an elastomer (polydimethylsiloxane) over the etched silicon surface. Finally, we generate a positive copy by casting one of a variety of polymers over the negative elastomer mold. We have demonstrated this replication process to an accuracy of less than 1 μm. The elastomer negatives can be reused, and the final polymer structures are rugged and cheap. Since the polymers are optically transparent, it is even possible to observe the flow dynamics in these microfluidic structures.

An example of a microfluidic structure fabricated by A. Young as part of the bioagent-detection program is shown in Figure B. This microfluidic component is designed to take in clumped biological particles that may be mixed with dirt or other contaminants, and, through a combination of chemical and mechanical processes, output declumped, purified biological particles. This microfluidic component features integrated microvalves, a multi-element turbulent microdisperser, several filter units, an enzyme storage tank, and several chemical reaction chambers. All these microcomponents are contained in a chip that is roughly 5 mm × 8 mm.

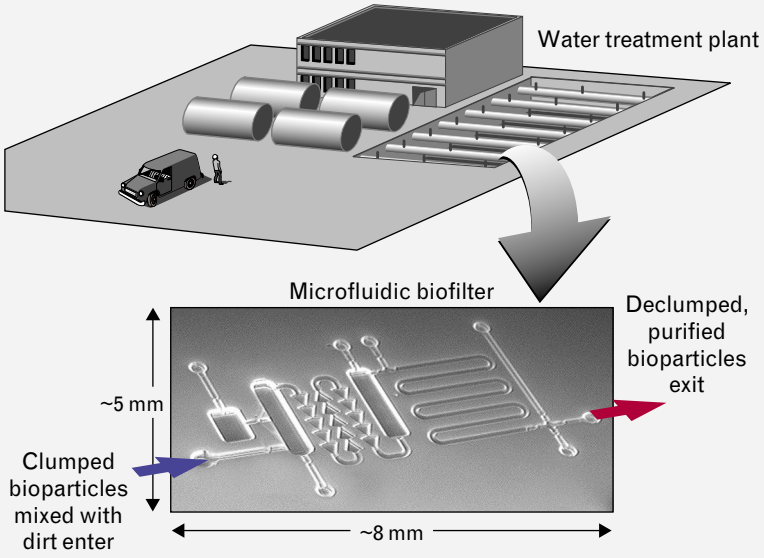

FIGURE B. Microfluidic biofilter. This microfluidic piece is designed to pre-filter biological particles before they are sent to an identifying sensor. The microfluidic biofilter is an extreme miniaturization of a conventional water-treatment plant.

The microfluidic structure in Figure B can be regarded as an extreme miniaturization of a waste treatment plant. The microfluidic structure does not have nearly the throughput of the waste-treatment plant, but it employs the same basic chemical and mechanical processes.

Reference
1. A.M. Young, T.M. Bloomstein, S.T. Palmacci, and M.A. Hollis, "Elastic-Membrane Microvalves for Microfluidic Network Integration," Solid State Research Report 1997:4, Lincoln Laboratory (23 Apr. 1997), DTIC #A342325.

the B-cell concept has the potential to develop into a rapid, sensitive, specific identifying sensor.

Future Bioagent Sensor Vision

Based on our technical progress thus far, we can easily envisage the sensor system shown in Figure 26. The system would include a network of miniature, low-power sensors. Each sensor would include a BAWS early-warning sensor and a B-cell identifying sensor, as well as Global Positioning System (GPS) and auxiliary sensors. The fully integrated sensor would be about the size of a large lunch box so it could easily be transported or mounted on a variety of platforms.

Information from the sensor would be instantly transmitted to a sophisticated data-fusion system and situational display, all housed in a laptop. With this system, a military chemical/biological officer or a civilian first-responder could interact with a network of stationary and mobile sensors and rapidly form an integrated picture of a bioagent attack. Such capability

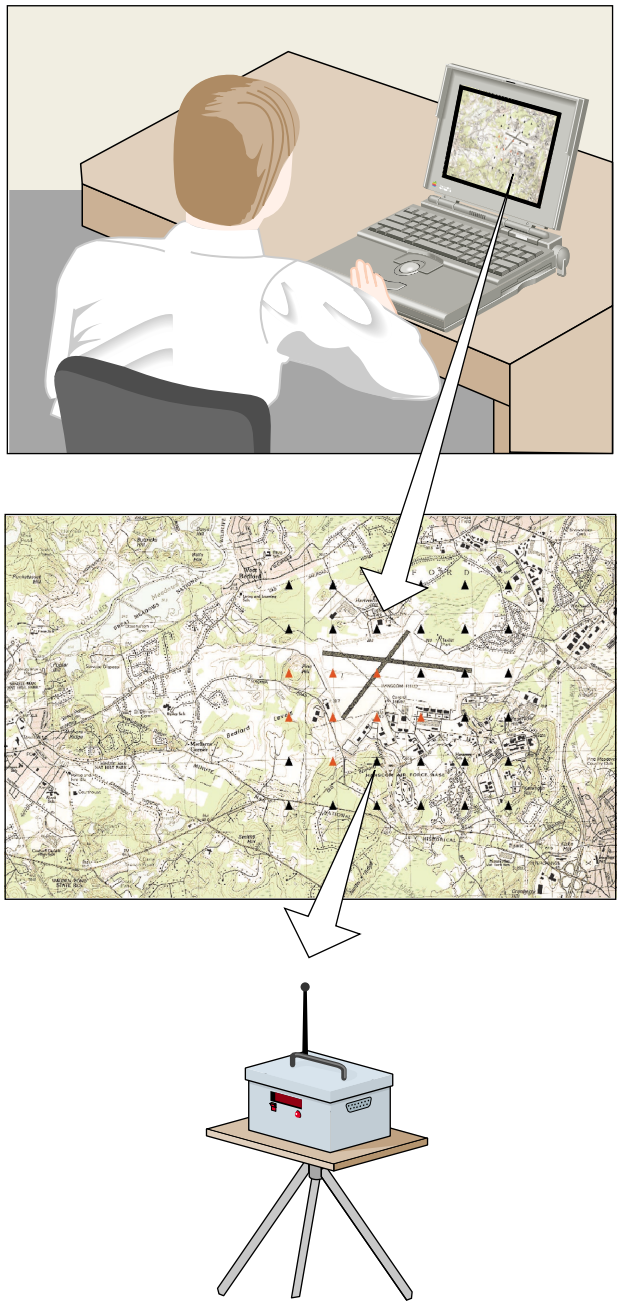

FIGURE 26. Possible future bioagent sensor system. This figure shows a network of integrated miniature low-power sensors. Each sensor would incorporate both an early-warning sensor and an identifying sensor.

could provide a significant technology advantage to the defensive side, helping to tip the balance from the current situation, where it appears that even a low-tech attacker has the advantage if he chooses to use biological weapons.

Acknowledgments

The research described in this article was conducted while I was program manager for Biological Warfare Defense at Lincoln Laboratory. The work was done by a large number of talented researchers from many different Divisions at Lincoln Laboratory. I thank everyone who contributed to the program, and I particularly acknowledge the following key researchers:

Roshan L. Aggarwal, Theodore M. Bloomstein, Robert P. Brady, Vincenzo Daneu, Salvatore Di Cecca, Herbert W. Feinstein, Darryl P. Greenwood, Mark A. Hollis, Thomas H. Jeys, Bernadette Johnson, Robert Kramer, Jae H. Kyung, Michael T. Languirand, Robert W. Miller, Frances Nargi, Michael E. O'Brien, Nathan R. Newbury, Lalitha Parameswaran, Ronald R. Parenti, Martha S. Petrovick, Todd H. Rider, Gregory S. Rowe, Ann E. Rundell, Antonio Sanchez-Rubio, Shen Y. Shey, Laura T. Bortolin, David P. Tremblay, Albert M. Young, and John Zayhowski.

I acknowledge Professor Jianzhu Chen and his colleagues in the MIT Department of Biology for their significant contributions to the B-cell based sensor. I also acknowledge Professor Harriet Burge and her colleagues at the Harvard School of Public Health for their significant contributions to the aerosol background measurements.

This research was supported by the U.S. Army, by the Defense Advanced Research Projects Agency (DARPA), by the Joint Program Office for Biological Defense, and by the Office of the Secretary of Defense. In the government sponsor community I particularly acknowledge Richard Smardzewski, Felix Reyes, and David Sickenburger from U.S. Army SBCCOM; not only did they provide funding for the BAWS sensor development, but they also were active participants in field tests involving the BAWS sensor.

I thank Darryl P. Greenwood, Mark A. Hollis, and Shen Y. Shey for providing helpful editorial comments on this article. Finally, I thank my secretary, Marjorie Banks, for her invaluable assistance in assembling this article.

REFERENCES

1. R.A. Falkennath, R.D. Newman, and B.A. Thayer, *America's Achilles Heel: Nuclear, Biological and Chemical Terrorism and Covert Attack* (MIT Press, Cambridge, Mass., 1998).
2. G.W. Christopher, T.J. Cieslak, J.A. Pavlin, and E.M. Eitzen, "Biological Warfare: A Historical Perspective," *J. Am. Med. A.* **278** (5), pp. 412–417.
3. P. Williams and D. Wallace, *Unit 731: Japan's Secret Biological Warfare in World War II* (Free Press, New York, 1989).
4. K. Alibeck with S. Handelman, *Biohazard* (Random House, New York, 1999).
5. Israel is a significant exception. Lists of signatories and nonsignatories are maintained by the SIPRI Chemical and Biological Warfare Project and may be found at the web page <http://projects.sipri.se/cbw/cbw-sipri-bradford.html>.
6. *Health Aspects of Chemical and Biological Weapons* (World Health Organization, Geneva, Switzerland, 1970).
7. U.S. Congress, Office of Technology Assessment, *Proliferation of Weapons of Mass Destruction: Assessing the Risks, OTA-ISC-559* (U.S. Government Printing Office, Washington, Aug. 1993).
8. The Australia Group list may be found at the web page <http://www.dtic.mil/mctl>, under section 3—Biological Technology.
9. Solid State Research Quarterly Technical Report 1998:1, Lincoln Laboratory (19 June 1998), DTIC #A347651.
10. Solid State Research Quarterly Technical Report 1998:2, Lincoln Laboratory (28 Oct. 1998), DTIC #A355512.
11. J.J. Zayhowski, "Passively Q-Switched Processor Microlaser," U.S. Patent No. 5,394,413 (28 Feb. 1995).
12. J.J. Zayhowski, "Passively Q-Switched Microchip Lasers and Applications," *Rev. Laser Eng.* **26** (12), 1998, pp. 841–846.
13. J.J. Zayhowski, "Q-Switched Microchip Lasers Find Real-World Applications," *Laser Focus World* **35,** Aug. 1999, pp. 129–136.
14. J.C. Bloch, B. Johnson, N. Newbury, J. Germaine, H. Memond, and J. Sinfield, "Field Test of a Novel Microlaser-Based Probe for *in Situ* Fluorescence Sensing of Soil Contamination," *Appl. Spectrosc.* **52** (10), 1998, pp. 1299–1304.
15. L.A. Condatore, Jr., R.B. Guthrie, B.J. Bradshaw, K.E. Logan, L.S. Lingvay, T.H. Smith, T.S. Kaffenberger, B.W. Jezek, V.J. Cannalito, W.J. Ginley, and W.S. Hungate, "U.S. Army Soldier and Biological Chemical Command Counter Proliferation Long Range–Biological Standoff Detection (CP LR-BSDS), *SPIE* **3707,** 1999, pp. 188–196.
16. B.J. Westand and M.F. Shlesinger, "On the Ubiquity of 1/f Noise," *Int. J. Mod. Phys. B* **3** (6), 1989, pp. 795–819.
17. T.H. Rider, "Optoelectronic Sensor," U.S. Patent Application Serial No. 08/987,410.
18. T.H. Rider and L.T. Smith, "Continuation in Part of Optoelectronic Sensor," U.S. Patent Application Serial No. 09/169/196.

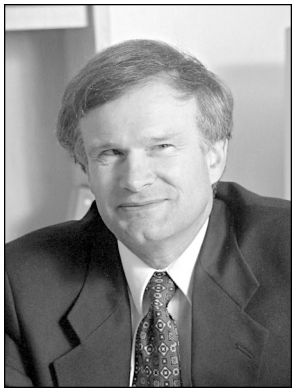

CHARLES A. PRIMMERMAN received an A.B. degree in physics from Duke University in 1968, and S.M. and Ph.D. degrees in nuclear engineering from MIT in 1970 and 1975, respectively. Immediately following graduate school he joined Lincoln Laboratory to work on adaptive optics, laser propagation, and high-energy-laser beam control. In 1984 when SDIO was formed, Dr. Primmerman was on loan to the Directed Energy Office, where he helped to establish new programs involving high-energy lasers for boost-phase intercept of ballistic missiles. In 1985 Dr. Primmerman returned to Lincoln Laboratory to become group leader. Until the fall of 1999 he directed a group involved in the development and field testing of advanced adaptive-optics and other electro-optical systems for high-energy-laser and laser-radar applications. Dr. Primmerman is particularly known for his pioneering work in the use of adaptive optics to compensate for atmospheric distortions. For this work he was corecipient of the 1993 SPIE Technology Achievement Award and in 1998 was named a Fellow of the Optical Society of America (OSA). In 1995 Dr. Primmerman helped initiate a new effort at Lincoln Laboratory involving the real-time detection of biological agents. He served as overall Program Manager for biological-warfare defense activities at Lincoln Laboratory until the fall of 1999. In the fall of 1999 Dr. Primmerman took a leave of absence from Lincoln Laboratory to take a temporary position in Washington with the Advanced Systems Concepts Office of the Defense Threat Reduction Agency. In his position as Special Assistant to the Director, Dr. Primmerman helps both to analyze emerging weapons-of-mass-destruction (WMD) threats and to develop counters to them. As escapes from the WMD world Dr. Primmerman enjoys downhill skiing and sailing his J/24.